A NEW METHOD TO

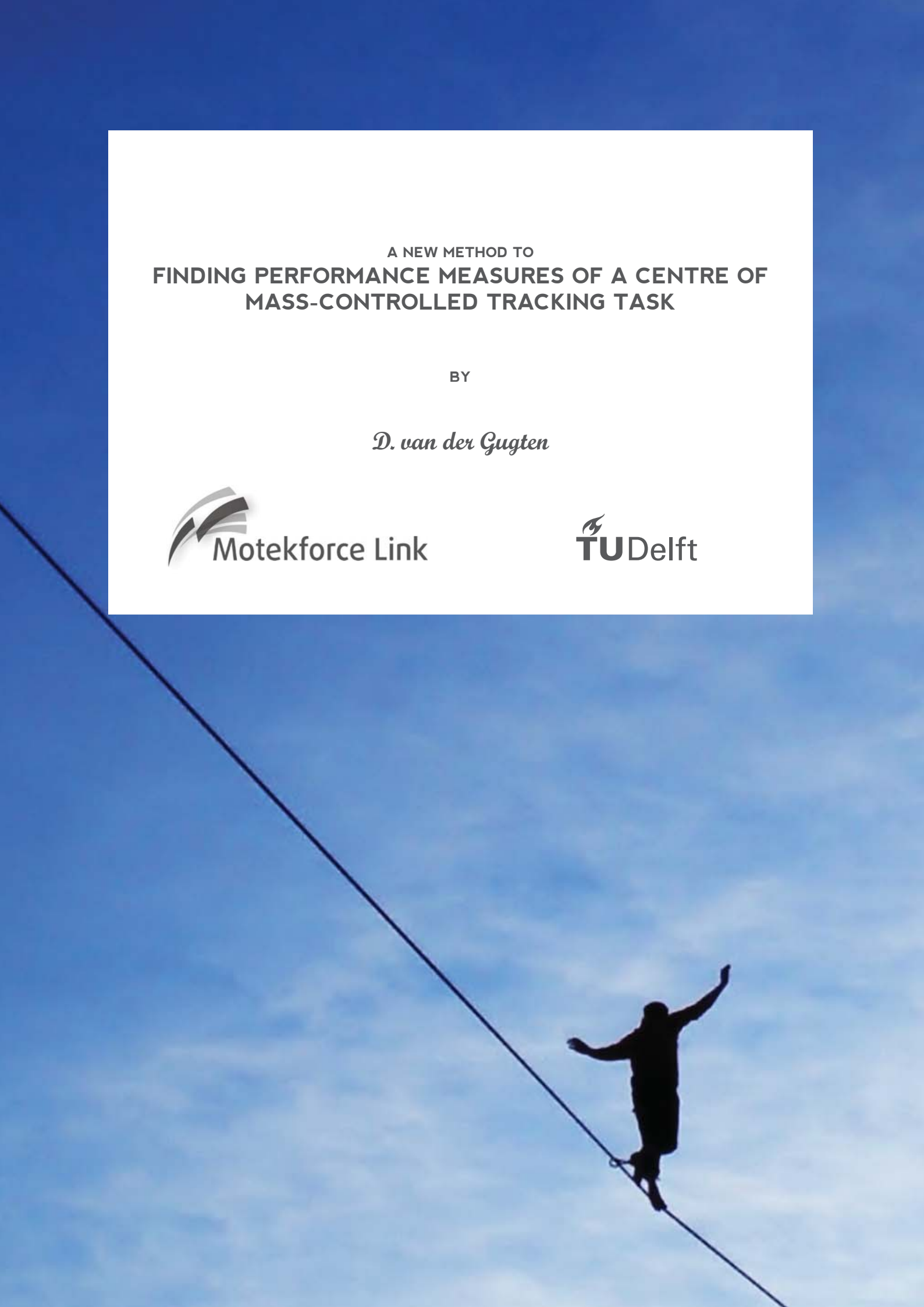
FINDING PERFORMANCE MEASURES OF A CENTRE OF MASS-CONTROLLED TRACKING TASK

BY

D. van der Gugten

Motekforce Link

TU Delft



This report is the result of the research conducted as a final assignment in graduating at the department of Biomedical Engineering of Delft University of Technology. In my research I examined the human balance system using equipment developed by Motekforce Link at the company's facility. A research conducted by Eduardo Cofré Lizama and Mirjam Pijnappels from VU University Amsterdam was used as basis and I am thankful for the information they shared.

I would like to thank Alfred Schouten, who was my supervisor on behalf of Delft University of Technology, for his patience and the nice and helpful meetings. I am grateful for the opportunity Motekforce Link gave me to conduct this research using their equipment, support and expertise. In particular, I would like to thank Frans Steenbrink, who supervised my project, and Sanne Roeles.

This research could not have been conducted without the help of the people from Motekforce Link who volunteered as test subjects, and I could not have finished the report without the help and support of friends and family, in particular my parents, Martin, Arnold and Liselot.

Dieke van der Gugten

Delft, April 16 2015

A new method to

Finding performance measures of a centre of mass-controlled tracking task

by

D. van der Gugten

in partial fulfillment of the requirements for the degree of

Master of Science
in Biomedical Engineering
specialisation Biomechatronics

at Delft University of Technology,
to be defended publicly on Friday May 29, 2015 at 12:45 AM.

Supervisor:	Dr. ir. A. C. Schouten
Thesis committee:	Dr. ir. M. M. van Paassen
	ir. J. H. Pasma

An electronic version of this thesis is available at http://repository.tudelft.nl/.

TU Delft Delft University of Technology

Abstract

This study focused on a new method to find accurate performance measures of a mediolateral centre of mass(CoM)-controlled visual tracking task, which might be sensitive enough to detect problems in balance control early on. Visual tracking tasks, controlled by mediolateral CoM displacement, have shown promising results in this respect [1], [2].
The task was performed by twenty-one healthy subjects who had to track an unpredictable horizontally moving target on the screen with a tracker which was controlled by mediolateral CoM displacement. The test was performed under three conditions: The CoM displacement was controlled by either a static gain, an integrator or a double integrator before the displacement of the tracker was displayed on the screen.
The results were analysed in the frequency domain. In this study the McRuer crossover-model [3], which was developed for aviation, was used to describe the frequency response of the participants while performing a visual tracking task in three test conditions. The three performance measures, the effective time delay $\tau_e[s]$, the crossover frequency $\omega_c[Hz]$ and the cutoff frequency $GX[Hz]$, were calculated from this estimator.
The overall coherence of the double integrator condition was extremely low, so these results were not taken into discussion. Nevertheless, the McRuer crossover model appeared to be a good descriptor for the frequency response of the subjects during balance-controlled visual tracking tasks in the static gain and integrator conditions. The test-retest reliability of the parameters was tested among nine of the subjects, no significant differences between the three tests were found.
The crossover frequency $\omega_c[Hz]$ and the cutoff frequency $GX[Hz]$, of both the static gain and integrator conditions have their advantages and disadvantages on behalf of the early detection of people at risk of falling. However, the two test conditions should be repeated with a larger subject group, as well as a subject group with known impaired balance, to find out which performance measure is the most accurate and sensitive to detect problems in balance early on.

Contents

1 Introduction **1**
1.1 Background . . . 1
1.2 MELBA . . . 1
1.3 Crossover-model . . . 2
1.4 Goal . . . 3
1.5 Hypothesis . . . 3

2 Methods **5**
2.1 Subjects . . . 5
2.2 Apparatus . . . 5
2.3 Task and procedure . . . 5
2.4 Data collection . . . 6
2.5 Data analysis . . . 6
2.5.1 Behaviour of the controlled element and the human frequency response . . . 6
2.5.2 Crossover model . . . 7
2.5.3 Repeatability / Test-retest . . . 8

3 Results **9**
3.1 Human Behaviour . . . 9
3.1.1 Time domain . . . 9
3.1.2 Frequency domain . . . 10
3.2 Crossover model . . . 12
3.2.1 Overview . . . 12
3.2.2 Parameter estimation . . . 12
3.2.3 Repeated-measures ANOVA . . . 15
3.3 Test-retest reliability . . . 16
3.3.1 Overview . . . 16
3.3.2 Parameter estimation . . . 16
3.3.3 Repeated-measures ANOVA . . . 16

4 Discussion **17**
4.1 Overview . . . 17
4.2 The McRuer Crossover Model . . . 17
4.2.1 General . . . 17
4.2.2 Condition 1 . . . 18
4.2.3 Condition 2 . . . 19
4.3 Test-Retest reliability . . . 20
4.4 Accuracy . . . 20
4.5 Recommendations . . . 21

5 Conclusion **23**

Bibliography **25**

A D-Flow Application **27**
A.1 Introduction . . . 28
A.2 Interface Application . . . 28

B Frequency response subjects **33**

C Test-retest parameter values **55**

List of Figures

1.1 Control scheme 2

2.1 The task 5

3.1 Raw data mean and standard deviation one trial single subject 9
3.2 Bode plot average controlled element $H(\omega)$ and human frequency response $G(\omega)$ . . . 10
3.3 Bode plot of crossover model fitted on one subject 12
3.4 Crossover frequency and cutoff frequency 13
3.5 Crossover frequency versus cutoff frequency 14

A.1 The application 28
A.2 The Runtime Console 29
A.3 The DRS window 30
A.4 The module groups 31

List of Tables

1.1 Expected frequency response of human balance control system 3
1.2 Values of the effective time delay and crossover frequencies 3

2.1 Overview task 6

3.1 Mean and standard deviation of estimated parameters 13
3.2 correlations of the crossover frequency versus the cutoff frequency 14
3.3 Results repeated-measures ANOVA 15
3.4 P-values 15
3.5 Results repeated-measures ANOVA test-retest 16

1

Introduction

1.1. Background

The body's ability to move in a specific direction or to maintain a certain pose while keeping equilibrium, such as keeping the centre of mass (CoM) above the base of support (BoS) [4] during quiet stance, while compensating for gravity and disturbance is known as balance control [5]. Balance control is a complicated and mainly unconscious process regulated by the nervous, motor and sensory systems. The sensory system comprises of vestibular, visual and proprioceptive subsystems. All the systems are interconnected and cooperative [6]. In daily life, the body's balance control mechanism is exposed to several disturbances, which can be divided into two types: external and internal [7]. External disturbance, such as uneven ground, gravity or other forces that have an impact on the body, as well as other environmental factors are very common. A healthy body is able to recover quickly from external disturbance. Noise in one or more of the systems or sensory inaccuracy is known as internal disturbance. These disturbances are always present, but a healthy body is able to cope with them.

If that is not the case, due to a defect or a deterioration in one of the systems involved in balance control, problems will occur with keeping balance. This might be attributable to a disease, trauma or ageing [8]. Particularly the elderly are frequently victim of an accident caused by balance problems, such as a fall, and this results in both direct and indirect costs. The direct costs are high; each year, 100.000 Accident and Emergency cases in the Netherlands are directly traceable to falls among the elderly, 48% of which indicated that physical problems such as vestibular or visual malfunctioning played a role. The total direct costs due to falls are estimated at €810.000.000 a year[1]. The indirect costs can be classified as trauma, immobilization and fear of renewed falls. Due to the ageing population, falls are becoming a growing matter of health concern and both direct and indirect costs will grow.

With current balance assessment methods, such as posturography, it is possible to locate balance problems and to train patients after a balance problem such as a fall has occurred. Balance problems can remain concealed for a long time because the (sub)systems involved in balance control are able to compensate for each other [9]. compensate each other. However, these systems cannot take over functions. If the system has deteriorated too much it will, in the end, lead to accidents. Current clinical tools are not sensitive enough to detect early stage impairments [6]. This study focuses on a diagnostic assessment method which might be sensitive enough to detect problems in balance control early on.

1.2. MELBA

This study elaborates on the studies perfomed by L.E. Cofré Lizama [1] on Mediolateral Balance Assessment (MELBA). He found a sensitive tool which is able to distinguish between young and older adults [2]. The tool is based on an assumption that the ability to accurately perform mediolateral CoM tracking deteriorates with age. Also mediolateral balance impairments have in particular been associated with an increased risk of falling in the elderly [1], [10], [11], [12]. A similar visual tracking task (VTT)

[1] Factsheet Valongevallen 55+, (http://www.veiligheid.nl/cijfers/valongevallen-55plussers - visited at 15-05-2015)

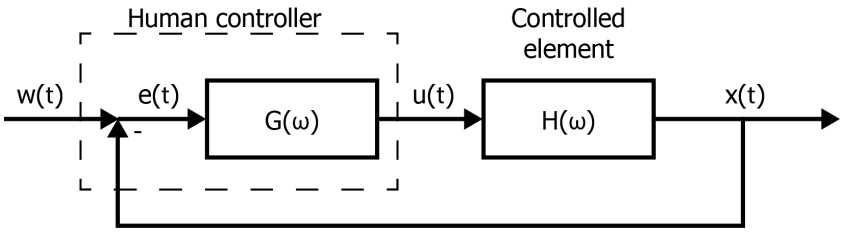


Figure 1.1: The simplified control scheme of a tracking task.

is used, in which the subject was instructed to track a target on the screen with a tracker controlled by the body's CoM position by gaining and interpreting the information from the screen. The subject then had to take action by using the position of the CoM as effector. The position data was analysed in the frequency domain. It shows the difference in magnitude and phase between the target and the tracker per frequency (of the target displacement). The performance measures of Cofré Lizama's study were the cutoff frequency $GX[Hz]$, the corresponding gain $GY[-]$, the frequency at which the phase "dropped" $PSX[Hz]$ and the corresponding phase $PSY[deg]$. These measures indicate to what frequency the subjects are able to track the target.

From an engineering perspective, this task is called a pursuit tracking task with the human balance control system as an element in a closed-loop control system [13]. This can be simplified to the control scheme shown in Figure 1.1 (compensatory tracking) where the two blocks represent the human balance control system $G(\omega)$ and the controlled element $H(\omega)$ and $w[t]$ is the input signal of the target, $u[t]$ is the measured mediolateral CoM displacement of the subject, $x[t]$ represents the output signal that controls the displayed tracker and $e[t]$ represents the error (or the difference) between signal $w[t]$ and $x[t]$. MELBA analyzed the performance of the closed loop, but this method does not necessarily provide information about the frequency response of the human balance control system $G(\omega)$ during the task.

1.3. Crossover-model

This study focuses on the open-loop frequency response of the human balance control system as an element of a control loop while performing a mediolateral CoM controlled visual tracking task. The frequency response of the human balance control as an element of a system has been described earlier by McRuer in his crossover model (1965) which was developed for aviation [3]. It is a convenient approximation suitable for many pilot-vehicle engineering purposes [14]. This model is based on the theory that human balance adapts to the system he is interacting with. It describes the open-loop frequency response near the crossover frequency ω_c of the human balance control system, while performing an *unpredictable* visual tracking task (Figure 1.1):

$$H_{OL}(\omega) = |G(\omega)H(\omega)| \doteq \frac{\omega_c}{j\omega} e^{-j\omega\tau_e} \tag{1.1}$$

$G(\omega)$ and $H(\omega)$ represent the transfer functions of the human frequency response and the controlled element. The right-hand part of the equation shows a delayed integrator. Since the human balance control system $G(\omega)$ adapts its frequency response to that of the controlled element $H(\omega)$, the open-loop frequency response of the human balance control system, while performing an unpredictable visual tracking task is expected to always be *a delayed integrator*. So for instance, if the controlled element is a static gain 1, the human frequency response would be an integrator $\frac{\omega_c}{j\omega} e^{-j\omega\tau_e}$. If it acts like an integrator $\frac{1}{j\omega}$, the human frequency response would be a delayed gain $Ke^{-j\omega\tau_e}$. both meaning that the open-loop system is an integrator according to Equation 1.1. Ultimately, if the controlled element is a double integrator $\frac{1}{(j\omega)^2}$, the human is expected to respond as a differentiator $j\omega\ \omega_c e^{j\omega\tau_e}$. *These three conditions are shown in Table 1.1 and will be examined in this study.*

Important measures of the study by McRuer were the effective time delay $\tau_e[s]$ and the crossover frequency $\omega_c[Hz]$. The effective time delay can be found in the transfer function of the human response $G(\omega)$. According to Stassen, it represents the sum of the neuromuscular time constant and the reaction

Table 1.1: The expected equalization adjustment of the human balance control system for various controlled elements.

$H(\omega)$	$G(\omega)$	Parameters
1	$\frac{\omega_c}{j\omega} e^{-j\omega\tau_e}$	$\tau_{lead} = 0$ $\tau_{lag} >> 1$
$\frac{1}{j\omega}$	$\omega_c e^{j\omega\tau_e}$	$\tau_{lead} = 0$ $\tau_{lag} = 0$
$\frac{1}{(j\omega)^2}$	$j\omega\ \omega_c e^{j\omega\tau_e}$	$\tau_{lead} >> 1$ $\tau_{lag} = 0$

Table 1.2: The values of τ_e, $\omega_c[Hz]$ and $GX[Hz]$ as measured by McRuer and Cofré Lizama [3], [1].

$H(\omega)$	τ_e	$\omega_c[Hz]$	$GX[Hz]$
1	0.33	0.80 to 0.95	1.34(0.32)
$\frac{1}{j\omega}$	0.36	0.68	
$\frac{1}{(j\omega)^2}$	0.50	0.53	

time constant, these values are more or less physiologically defined [13]. The values of the neuromuscular time constant $\tau_n \simeq 200msec$ and the reaction time constant $\tau_v \simeq 120 - 200msec$. This range shows the difference in reaction time between a simple (short reaction time) and a difficult system (long reaction time). So it the effective time delay is expected to have a value $\tau_e = \tau_n + \tau_{(v)} \simeq 320 - 400msec$. The values as measured by McRuer are in the same range as shown in Table 1.2.

The performance of the human frequency response is described with the system bandwidth, which indicates the frequency range for which the tracking errors are small. This range are the frequencies between 0 Hz and the crossover frequency $\omega_c[Hz]$. The larger $\omega_c[Hz]$, the better the performance. The crossover frequency $\omega_c[Hz]$ is the value for which the gain of the open-loop response $|G(\omega)H(\omega)| = 1$. Since the effective time delay is more or less physiologically defined, the human balance system will not have the ability to accurately track all frequencies. The performance is strongly dependent on the form of the controlled element as can be seen in Table 1.2. The crossover frequency $\omega_c[Hz]$ appears to be an accurate and sensitive measure. Since the study by McRuer was performed by trained fighter pilots with a joystick as a controller, it is unknown whether the crossover model also applies to mediolateral CoM-displacement-controlled visual tracking tasks.

The cutoff frequency $GX[Hz]$ of MELBA is comparable to the crossover frequency $\omega_c[Hz]$ of McRuer [1], [3]. However, it is calculated from the closed-loop transfer function equal to $GY[-]$ instead of that of the open-loop equal to one. Furthermore, the controlled element $H(\omega)$ of MELBA is a static gain only. The value of $GX[Hz]$ is shown in Table 1.2 as well [3].

1.4. Goal

The goal of this study was to find out whether a mediolateral centre of mass-controlled visual tracking task, provides accurate performance measures. The goal is to be reached by addressing the following questions:

1. Is the McRuer crossover model able to describe the human frequency response during a mediolateral CoM displacement-controlled visual tracking task?
2. Is the protocol test-retest reliable?
3. Which parameter, the effective time delay $\tau_e[s]$, the crossover frequency $\omega_c[Hz]$ or the cutoff frequency $GX[Hz]$, in what condition, might be an accurate performance measure?

1.5. Hypothesis

It is expected that the McRuer crossover model is applicable for centre of mass-controlled tracking tasks. Furthermore, the expectation is that the effective time delay $\tau_e[s]$ will be the lowest for condition 1 and the highest in condition 3. The crossover frequency $\omega_c[Hz]$ and cutoff frequency $GX[Hz]$ will be highest for condition 1 and lowest for condition 3. However, if the condition is too complex, the subjects will not be able to track the target at all. Then, it is impossible to estimate the performance measures.

2

Methods

2.1. Subjects

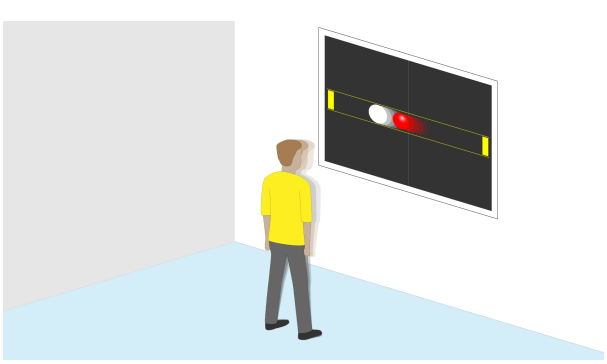
Twenty-one healthy participants, 14 men and 7 women (age of 42 ± 20 years; height $1.79 \pm .21$ m) participated in the first test of this study. Nine of these participants, 5 men and 4 women (age of 45.5 ± 19.5 years; height $1.76 \pm .18$ m) also performed in the second and third test which took place 2 ± 0 and 34.5 ± 1.5 days after the first test.

2.2. Apparatus

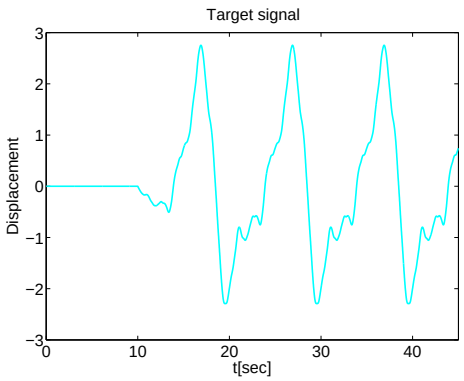
At the beginning of the first test, the task was explained briefly and the length of the participant was measured. They were positioned at 1.5 m distance from a screen (150 x 140cm) on socks with their arms on their backs and their heels on the floor. The stance width, which is the width of the BoS, was standardized to an intermalleoli distance of 8% of the body height to prevent the lower limb neuromechanical responses to vary [15], [16]. The maximum required centre-to-side displacement of the CoM was $1/2$ stance width, allowing the mediolateral CoM displacements to be within the base of support. This was maximum amplitude of the tracker during static gain, and therefore the maximum amplitude of the target as well.

2.3. Task and procedure

Each participant performed a series of visual tracking tasks (VTT) in similar order. The participant's task was to track the target, represented by a white sphere, with a tracker, displayed by a red sphere as shown in Figure 2.1a. The target was controlled by a signal consisting of of the sum of nine sine waves containing the frequencies 0.1, 0.2, 0.3, 0.5, 0.7, 1.0, 1.4, 2.0, and 3.0 Hz with descending



(a) The test set-up



(b) The multi sine controlling the target

Figure 2.1: The task

Table 2.1: An overview of the task protocol

Condition	$H(\omega)$	Trials				Outline single trial
1	1	1	**2**	**3**	**4**	10s quiet stance -
2	$\frac{1}{j\omega}$	1	**2**	**3**	**4**	5s increase from 0 to normal -
3	$\frac{1}{(j\omega)^2}$	1	**2**	**3**	**4**	**30s trial** - 10s rest

amplitudes and random phases for each trial. The frequencies were chosen in such a way that one trial contained three identical cycles of 10 s. The VTT was divided into three conditions; either the static gain (condition 1), the integrator (condition 2) or the double integrator (condition 3) of the participant's CoM position data was displayed by the tracker. Each condition consisted of four trials of 45 s with 10 s rest in between trials, so the total test consisted of 12 trials of 45 seconds. The first 10 s of the trials were not recorded, thereafter the amplitude of the multi sine controlling the target increased from 0 to normal in 5 s as is shown in Figure 2.1b so that the participant could get used to the tracker's reaction to CoM movement and tracking the target. An overview of this procedure is shown in Table 2.1; the bold text are the parts that will be analysed.

2.4. Data collection

The COM data was obtained with three markers on the left and right anterior superior iliac spine and the sternum, and four Vicon Bonita cameras with Tracker 2.0. D-flow v3.18.2 (MotekForce Link, Amsterdam, the Netherlands) was used to construct the target signal, display the target, calculate and display the position of the tracker and collect the data with a sample frequency of 100 Hz. The target and tracker data were collected as well as the raw COM position. A description of the D-Flow application can be found in Appendix A.

2.5. Data analysis

To answer the questions about the human frequency response during a tracking task, the data (n=21) was examined. The question about the learning effect was answered with the use of the data from the nine subjects that performed both test 1, 2 and 3. All data analysis was performed in Matlab R2012b (Mathworks, Natick MA, U.S.A.). The statistic analysis was performed with IBM SPSS Statistics 22 (IBM Corporation, Armonk NY, U.S.A.).

The response of both the controlled element and the human balance control system was analysed in both the time and frequency domain. This section describes what steps were taken to calculate the results.

2.5.1. Behaviour of the controlled element and the human frequency response

Time domain

The sample time of the D-Flow software is partially dependent on the performance of the computer. Therefore, the data had to be re-sampled first by interpolating the data of each trial at 100 Hz between 0 and 45 seconds to equally distribute the data in time. Then, the first five seconds of each trial were deleted and the first trial of each section was also removed from data, resulting in 3x3 trials of 30 seconds each for each subject. Thereafter each trial was divided into three cycles of ten seconds.

Frequency domain

To be able to estimate the frequency response function (FRF), the cross-spectral- (2.1-2.3) and power-spectral densities (2.4) had to be calculated. These are the Fourier Transform of the signal's cross- and autocorrelation and describe how the variance of the input data is distributed over the frequency spectrum.

$$S_{wu}(\omega) = \frac{1}{T} W^* U \tag{2.1}$$

$$S_{we}(\omega) = \frac{1}{T} W^* E \tag{2.2}$$

$$S_{wx}(\omega) = \frac{1}{T} W^* X \tag{2.3}$$

$$S_{ww}(\omega) = \frac{1}{T} |W(f)|^2 \tag{2.4}$$

Where $T(s)$ is the cycle time, $U[f]$, $E[f]$ and $X[f]$ are the Lapace transforms of the datasets $u[t]$, $e[t]$ and $x[t]$. $W^*[f]$ and $|W[f]|$ are the complex conjugate and the absolute values of the Laplace transform of $w[t]$.

The spectral densities of the nine cycles of each condition were averaged per subject. The freqency response of each subject $G(\omega)$ in the frequency domain was estimated with Equation 2.6. For the averaged estimated frequency response of the human $\hat{G}(\omega)$ and controlled element $\hat{H}(\omega)$, the spectral densities of all subjects were averaged before the frequency response was estimated by Equations 2.5 and 2.6.

$$\hat{H}(\omega) = \frac{S_{wx}}{S_{wu}} \tag{2.5}$$

$$\hat{G}(\omega) = \frac{S_{wu}}{S_{we}} \tag{2.6}$$

The coherence of the human frequency response (Equation 2.7) and the controlled element (Equation 2.8) was calculated as well.

$$\gamma_{wu}(\omega) = \frac{S_{wu}^2}{S_{ww} S_{uu}} \tag{2.7}$$

$$\gamma_{wx}(\omega) = \frac{S_{wx}^2}{S_{ww} S_{xx}} \tag{2.8}$$

The open- and closed-loop frequency response was estimated with Equations 2.9 and 2.10.

$$\hat{H}_{OL}(\omega) = |\hat{G}\omega H\omega| = \frac{S_{wx}}{S_{we}} \tag{2.9}$$

$$\hat{H}_{CL}(\omega) = \frac{\hat{G}\omega H\omega}{1 + \hat{G}\omega H\omega} = \frac{S_{wx}}{S_{ww}} \tag{2.10}$$

The FRF describes the relation between the in- and output of a system in the frequency domain. They will be represented in a figure, showing the gain and phase differences per frequency.

2.5.2. Crossover model

Parameter estimation

$$G(\omega) = K \frac{1 + j\omega\tau_{lead}}{1 + j\omega\tau_{lag}} e^{-j\omega\tau_e} \tag{2.11}$$

To estimate the response of the subjects according to the crossover model (1.1), the gain $K[-]$, time contants $\tau_{lead}[s]$ and $\tau_{lag}[s]$ and the effective time delay $\tau_e[s]$ of the FRF (Equation 2.11) for the three conditions were estimated for each subject. A nonlinear least-squares problem solver was used to minimize the difference between the estimation (2.6) and the model (2.11), including the coherence to not rely on noisy data: $\sqrt{\gamma}|\log(G/\hat{G})$. The expected values of these parameters for each condition were shown in Table 1.1.

Crossover frequency and cutoff frequency

The crossover frequency $\omega_c[Hz]$ is the frequency for which the magnitude of the open-loop crossover model (Equation 1.1) $|\hat{G}(\omega)H(\omega)| = 1$ [3]. $\hat{G}(\omega)H(\omega)$ was calculated by multiplying the mean estimated human model $\hat{G}(\omega)$ by the real $H(\omega) = 1$, $H(\omega) = \frac{1}{j\omega}$ and $H(\omega) = \frac{1}{(j\omega)^2}$. Thereafter the absolute values were solved for 1, resulting in the crossover frequency $\omega_c[Hz]$.

The cuttoff frequency $GX[Hz]$ is the frequency for which the closed-loop gain $\frac{\hat{G}\omega H\omega}{1+\hat{G}\omega H\omega}$ was 70% of the average of the three maximum gain values [1].

2.5.3. Repeatability / Test-retest

Parameter estimation

The parameters of the nine subjects of the three tests were calculated in the same way as described in Section 2.5.2. Also the means and standard deviations were calculated.

ANOVA

To analyse the test-retest reliability of this study, a repeated-measures ANOVA was performed for each of the estimated parameters K, τ_{lead}, τ_{lead} and τ_e of all subjects as well as for the performance measures ω_c and GX. If the assumption of sphericity was violated, the value of F was corrected with the Greenhouse-Geisser adjustment.

3 Results

3.1. Human Behaviour

In order to discuss the estimated frequency response of the subjects $\hat{G}(\omega)$ during an unpredictable tracking task while interacting with three different controlled elements $H(\omega) = 1$ (condition 1), $H(\omega) = \frac{1}{j\omega}$ (condition 2) and $H(\omega) = \frac{1}{(j\omega)^2}$ (condition 3), this section shows the results in the time and frequency domain. The crossover model (1.1) was used to estimate the system descriptors [3]. The performance measures were calculated from the system described by the model. Statistic analysis was performed to analyse the test-retest ability of the test protocol.

3.1.1. Time domain

Figure 3.1 shows the means and the standard deviations of cycles of 10 seconds of all of the raw signals $w[t]$, $e[t]$, $u[t]$ and $x[t]$ of one trial of a single subject. When looking at these plots, a couple of characteristics can easily be derived.

The frequencies of the target signal $w(t)$ were chosen as such that the signal could be divided in three identical cycles as can be seen by the absence of the standard deviation of the plots in the first column of the figure.

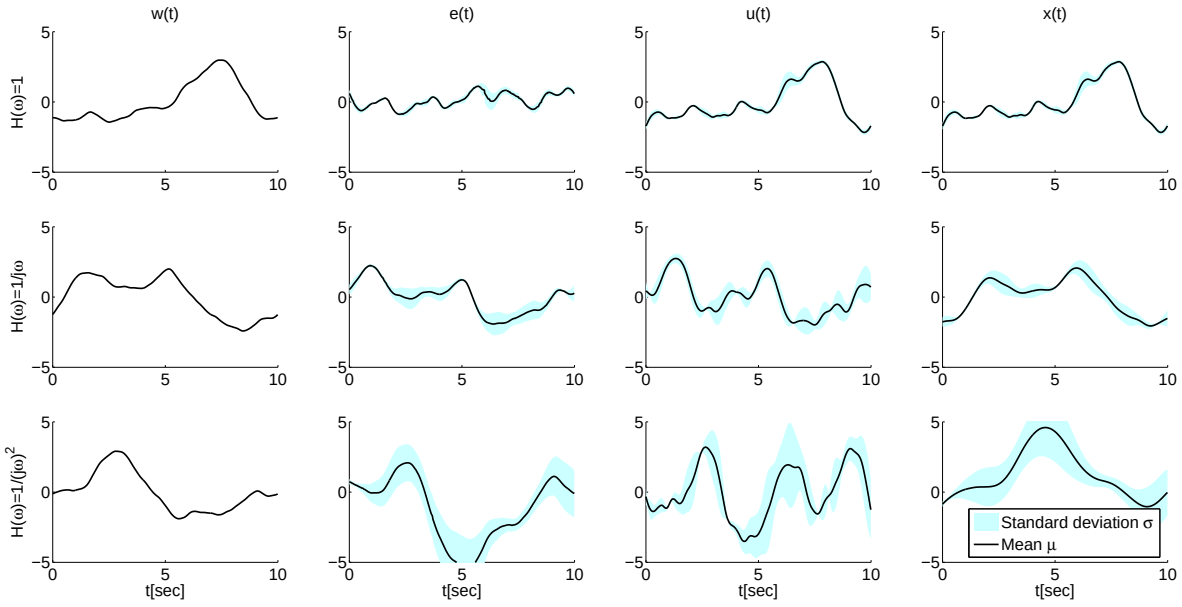


Figure 3.1: The means and standard deviations of three cycles of one trial of a single subject.

It is also notable that the standard deviation of the signals $e[t]$, $u[t]$ and $x[t]$ of condition 1 is the lowest and that of condition 3 is the highest. This implicates that the subject's mediolateral CoM displacement as a reaction to the displacement of the target is relatively constant during condition 1, deviates a little during condition 2 and has a large deviation during condition 3.

Furthermore, for the fluctuation of the error signal $e[t]$ yields the as for the standard deviation, meaning that the overall difference between the target $w[t]$ and the tracker $x[t]$ is larger when interacting with the integrator and double integrator compared to interacting with the static gain.

3.1.2. Frequency domain

The estimated frequency response functions (FRF's) of the system elements will be represented by a gain and phase plot. Each FRF is accompanied by a coherence plot. The coherence is a measure for the linearity and the amount of noise at each frequency in the FRF. The coherence has a value between zero and one for each frequency. A high coherence indicates linearity of the frequency response as well as low noise in the output signal. If the coherence value decreases, noise takes prominence on the estimated frequency response. The higher the coherence, the more reliable the estimate of the transfer function. An extremely low coherence might indicate that the estimation is not reliable.

First the FRF's of the averaged (over all subjects) estimated response of the human balance control system $\hat{G}(\omega)$ and controlled element $\hat{H}(\omega)$ will be shown. Second the FRF of a single subject is represented, accompanied by the estimated from the crossover model. At last, the open- and closed-loop FRF's can be seen.

Figure 3.2 shows the FRF's of the averaged (over all subjects) estimated response of the human $\hat{G}(\omega)$ and controlled element $\hat{H}(\omega)$ (solid line) as well as the real systems (dotted line). The red, green and blue colour represents condition 1, 2 and 3. The FRF's plotted in this figure are calculated from the average spectral densities of all subjects. This figure is to give an overview of the frequency response of both system elements.

The first thing that stands out in both the estimated FRF of the human balance control system $\hat{G}(\omega)$ and that of the controlled element $\hat{H}(\omega)$ is the decreasing coherence for increasing frequencies as well as an overall lower coherence for condition 2 and even more for condition 3 compared to that of condition 1. The extremely low coherence of the FRF of condition 3 also suggests invalidity of these results.

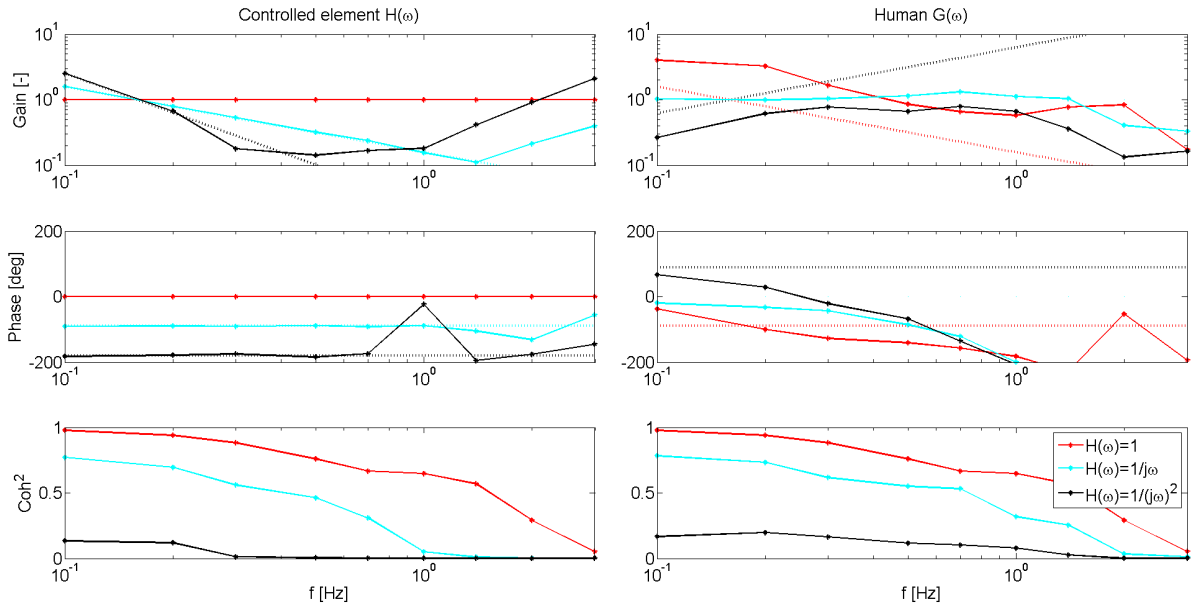


Figure 3.2: A magnitude, phase and coherence plot of the frequency response of the human $G(\omega)$ (right) and the controlled element $H(\omega)$ (left)

In the left half of the figure, the estimator of the controlled element $\hat{H}(\omega)$ is plotted. To compare the estimated systems with the pure systems, the pure systems static gain 1, integrator $\frac{1}{j\omega}$ and double integrator $\frac{1}{(j\omega)^2}$ are shown as well. For the static gain $\hat{H}(\omega) = 1$ it is expected that the gain will be equal to 1 and the phase $0\,\mathrm{deg}$ for all frequencies, from the figure can be seen that this is true. For an integrator $\hat{H}(\omega) = \frac{1}{j\omega}$, the gain has to decrease with $-1/dec$ and the phase constantly has to be $-90\,\mathrm{deg}$; for a double integrator a gain of $-2/dec$ and a phase of $-180\,\mathrm{deg}$ are predicted. What can be seen from these plots is that the average frequency response of the controlled element $\hat{H}(\omega)$ is comparable with the pure systems of a static gain 1, an integrator $\frac{1}{j\omega}$ and a double integrator $\frac{1}{(j\omega)^2}$, suggesting that the systems can be regarded as such. It should be noted however, that for increasing frequencies the difference between the estimated system and the measured system responses increases. This can be regarded to the decreasing coherence for increasing frequencies.

According to the crossover model (Equation 1.1), the product of the human frequency response $G(\omega)$ and the controlled element $H(\omega)$ should always be an integrator, as discussed in 1.3. So while interacting with the controlled element that responds like a static gain $H(\omega) = 1$, the human balance control system is expected to respond like a delayed integrator $G(\omega) = \frac{\omega_c}{j\omega} e^{-j\omega\tau_e}$ (gain equal to 1 and phase equal to $0\,\mathrm{deg}$). While interacting with an integrator $H(\omega) = \frac{1}{j\omega}$, the human balance control system is expected to respond like a delayed static gain $G(\omega) = \omega_c\, e^{j\omega\tau_e}$ (gain slope $-1/dec$ and phase equal to $-90\,\mathrm{deg}$) and while interacting with a double integrator $H(\omega) = \frac{1}{(j\omega)^2}$, the human balance control system is expected to respond like a delayed differentiator $G(\omega) = j\omega\ \omega_c e^{j\omega\tau_e}$ (gain slope $+1/dec$ and phase equal to $90\,\mathrm{deg}$). To compare the estimated systems with the pure systems, a pure integrator $\frac{1}{j\omega}$, static gain 1 and differentiator $\frac{j\omega}{1}$ are represented in the figure by the red, green and blue dotted lines in the right magnitude and phase plots, the estimated human reponse $\hat{G}(\omega)$ is represented by the solid lines in identical colours. The estimated response of the static gain $\hat{G}(\omega) = \omega_c\, e^{j\omega\tau_e}$ is comparable with that of the pure static gain. However, what stands out is that both the estimated integrator $\hat{G}(\omega) = \frac{\omega_c}{j\omega} e^{-j\omega\tau_e}$ and differentiator $\hat{G}(\omega) = j\omega\ \omega_c e^{j\omega\tau_e}$ are shifted compared to the pure systems, while the form is comparable. This is the result of a gain unequal to zero. The phase of the three plots is approximately the right value at low frequencies. It decreases for increasing frequency, this is caused by the time delay.

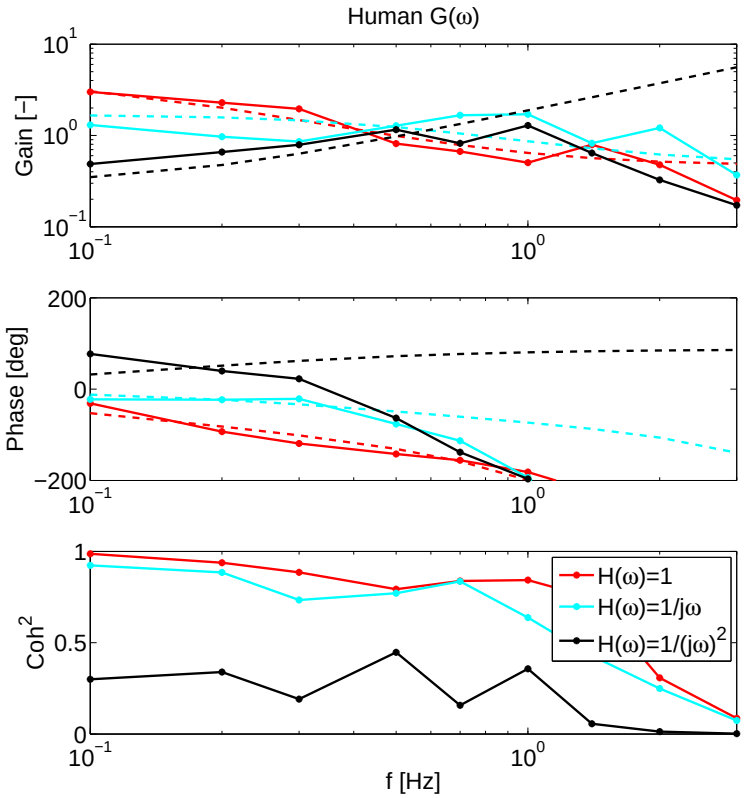


Figure 3.3: The magnitude, phase and coherence of the FRF of one subject

3.2. Crossover model

3.2.1. Overview

This section shows to what amount McRuer crossover model [3] is able to describe the human frequency response $G(\omega)$. First, the fitted parameters and the crossover frequencies $\omega_c[Hz]$ and cutoff frequencies $GX[Hz]$ are shown. Second, it will be verified whether the parameters do significantly differ from each other.

3.2.2. Parameter estimation

Figure 3.3 shows an example of fitting Equation 2.11 on the transfer function of the measured data on one subject in order to estimate the four parameters of the gain K, time constants τ_{lead} and τ_{lag} and effective time delay τ_e. This is done for each subject interacting with each controlled element $H(\omega) = 1$, $H(\omega) = \frac{1}{j\omega}$ and $H(\omega) = \frac{1}{(j\omega)^2}$. The measured transfer functions are shown by the solid lines and the fitted model is represented by the dashed lines. The red, green and blue colour represents condition 1, 2 and 3. The figures of the estimation of the crossover model onto the other 20 subjects can be found in Appendix B.

Because the fitting was weighed with the coherence, the model prevails for decreased coherence and the fit gets worse. Furthermore, it appears that this subject responds as expected: Like an integrator $G(\omega) = \frac{\omega_c}{j\omega} e^{-j\omega\tau_e}$ when interacting with a static gain, a static gain $G(\omega) = \omega_c e^{j\omega\tau_e}$ when interacting with an integrator and a differentiator $G(\omega) = j\omega\ \omega_c e^{j\omega\tau_e}$ when interacting with a double integrator. One can see that the estimated models are a fairly well fit, however, for both the magnitude and the phase the fitted model diverges from the measured data due to the decreasing coherence for increasing frequency.

Table 3.1: The means and the standard deviation of the estimated parameters, the crossover and cutoff frequencies (n=21).

$H(\omega)$	$K[-]$	(SD)	$\tau_{lead}[s]$	(SD)	$\tau_{lag}[s]$	(SD)	$\tau_e[s]$	(SD)
1	12.11	(10.51)	0.11	(0.07)	3.25	(2.34)	0.33	(0.13)
$\frac{1}{j\omega}$	1.38	(0.57)	0.20	(0.29)	0.35	(0.22)	0.30	(0.23)
$\frac{1}{(j\omega)^2}$	0.19	(0.15)	4.58	(3.66)	0.56	(0.35)	0.27	(0.28)

$H(\omega)$	$\omega_c[Hz]$	(SD)	$GX[Hz]$	(SD)
1	0.61	(0.13)	1.24	(0.54)
$\frac{1}{j\omega}$	0.20	(0.06)	0.39	(0.09)
$\frac{1}{(j\omega)^2}$	0.10	(0.03)	0.19	(0.03)

The mean values and the standard deviations of the estimated four parameters $K[-]$, $\tau_{lead}[s]$, $\tau_{lag}[s]$ and $\tau_e[s]$ of all 21 subjects are displayed in Table 3.1.

The mean value of the gain K is the highest for condition 1 and the lowest for condition 3. The values of time constant $\tau_{lead}[s]$ are approximately zero seconds for condition 1 and 2 and 4.58 seconds for condition 3. The values of time constant $\tau_{lag}[s]$ are 3.25 seconds for condition 1 and approximately zero for condition 2 and 3. The values of the effective time constant are on average 0.30 seconds, but that of condition 1 is the lowest and that of condition 3 the highest. Logically, the values of the parameters are more widely distributed when the mean is higher.

Table 3.1 also shows both the mean values and standard deviations for the crossover frequency $\omega_c[Hz]$ as calculated by McRuer and GX as calculated by Cofré Lizama [1]. These values are calculated for each subject using the crossover model. The values of $GX[Hz]$ are approximately twice the value of the crossover frequency $\omega_c[Hz]$. The values are highest for condition 1 and lowest for condition 3.

Figure 3.4 shows the open- and closed-loop FRF's estimated from both the crossover model (solid line) and the spectral densities (dotted line) $H_{OL} = |\hat{G}(\omega)H(\omega)| = \frac{S_{wx}}{S_{we}}$ and $H_{CL} = \frac{\hat{G}(\omega)H(\omega)}{1+\hat{G}(\omega)H(\omega)} = \frac{S_{wx}}{S_{ww}}$ of one subject. The red, green and blue colour represents condition 1, 2 and 3. The figures of the other 20 subjects can be found in Appendix B.

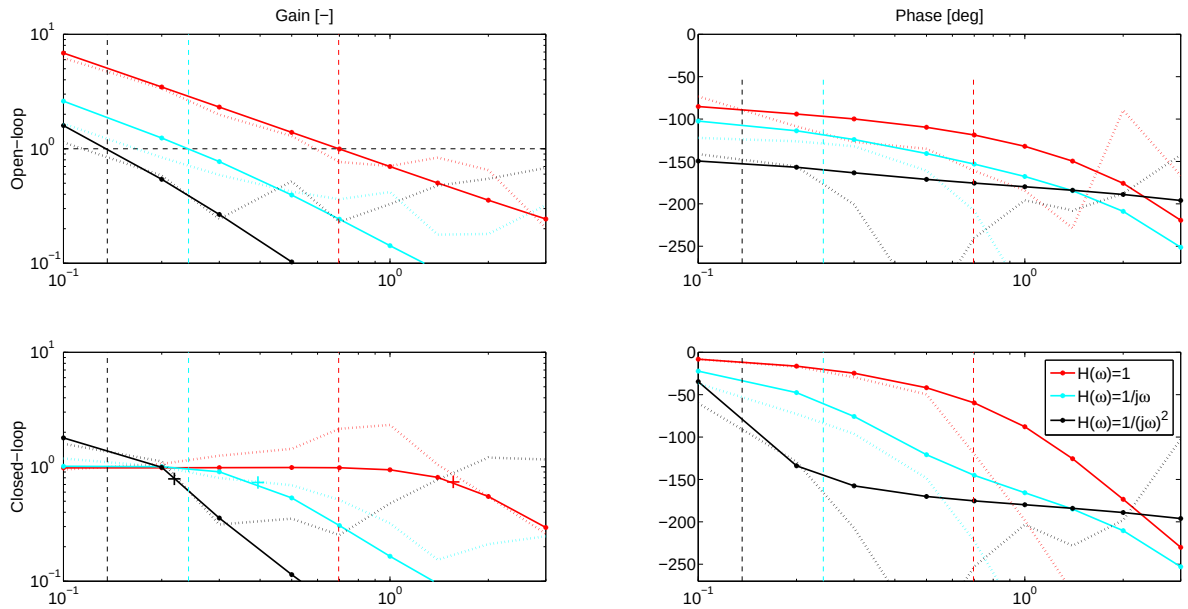


Figure 3.4: The open- and closed-loop magnitude and phase plot, showing the crossover frequency ω_c and the cutoff frequency GX

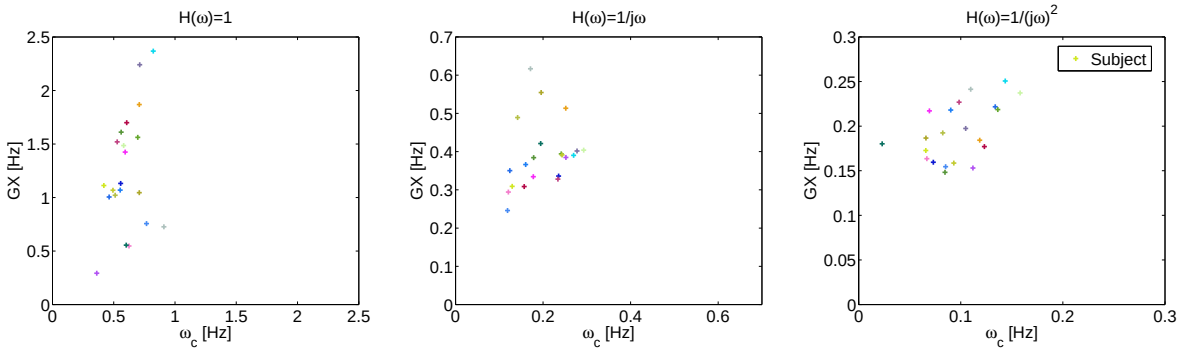


Figure 3.5: The crossover frequency ω_c versus the cutoff frequency GX per condition per subject

Table 3.2: The correlations of the crossover frequency ω_c versus the cutoff frequency GX per condition

$H(\omega)$	Pearson Correlation	Sig. (2-tailed)
1	0.329	0.073
$\frac{1}{j\omega}$	0.251	0.273
$\frac{1}{(j\omega)^2}$	**0.519**	0.016

The FRF's calculated from the spectral densities are similar to those calculated from the fitted models for the lower frequencies. One can see that all three open loop FRF's calculated from the crossover model approximately responds like an integrator. The crossover frequencies, that indicate to what frequency a subject is able to track the target, are calculated where the open-loop FRF is equal to one; these values are displayed by the dashed line in both the open-loop and the closed-loop gain plots. One can see that the crossover frequency approximately corresponds with the break points of the closed loop FRF's. In the closed-loop gain plot, GX is also plotted as displayed by the black plus-signs. It can be seen that these values lay on the plots however, compared to the crossover frequencies, the values are higher for a lower gain.

Figure 3.5 shows whether the crossover frequency ω_c and the cutoff frequency GX of each condition correlate. According to Table 3.2, only the correlation of condition 3 is significant at the 0.05 level.

Table 3.3: The exact significance levels for the F-ratios the difference between the estimated parameters, the crossover and cutoff frequencies. *(* assumption of sphericity was violated ($p < .05$), the value of F is corrected with the Greenhouse-Geisser adjustment [17])*

$K[-]$	$\tau_{lead}[s]$	$\tau_{lag}[s]$
$F(1.004, 20.085) = 24.827$ * $p = .000$	$F(1.008, 10.151) = 31.416$ * $p = .000$	$F(1.046, 20, 926) = 30.557$ * $p = .000$

$\tau_e[s]$	$\omega_c[Hz]$	$GX[Hz]$
$F(1.541, 30.828) = .284$ * $\mathbf{p = .697}$	$F(1.213, 24.259) = 235.470$ * $p = .000$	$F(1.036, 20.719) = 66.627$ * $p = .000$

Table 3.4: P-values of the significant differences of the estimated parameters between the three conditions.

$H(\omega)$		$K[-]$	$\tau_{lead}[s]$	$\tau_{lag}[s]$	$\tau_e[s]$	$\omega_c[Hz]$	$GX[Hz]$
1	$\frac{1}{j\omega}$	$p = .000$	$\mathbf{p = .308}$	$p = .000$		$p = .000$	$p = .000$
	$\frac{1}{(j\omega)^2}$	$p = .000$	$p = .000$	$p = .000$		$p = .000$	$p = .000$
$\frac{1}{j\omega}$	1	$p = .000$	$\mathbf{p = .308}$	$p = .000$		$p = .000$	$p = .000$
	$\frac{1}{(j\omega)^2}$	$p = .000$	$p = .000$	$\mathbf{p = .083}$		$p = .000$	$p = .000$
$\frac{1}{(j\omega)^2}$	1	$p = .000$	$p = .000$	$p = .000$		$p = .000$	$p = .000$
	$\frac{1}{j\omega}$	$p = .000$	$p = .000$	$\mathbf{p = .083}$		$p = .000$	$p = .000$

3.2.3. Repeated-measures ANOVA

Table 3.3 shows the results of the repeated-measures ANOVA for each parameter. All parameters differ significantly from each other except for the effective time delay $\tau_e[s]$. Taking a closer look at the differences between the other parameters in Table 3.4 one can see that the value of $\tau_{lead}[s]$ for the double integrator is significantly different from the values of the static gain and integrator, which do not significantly differ from each other. Also the value of $\tau_{lag}[s]$ for the static gain is significantly different from the values for the integrator and double integrator.

Table 3.5: The exact significance levels for the F-ratios of the estimated parameters, the crossover and cutoff frequencies of the three conditions for three tests. *(* assumption of sphericity was violated ($p < .05$), the value of F is corrected with the Greenhouse-Geisser adjustment [17])*

$H(\omega)$	$K[-]$	$\tau_{lead}[s]$	$\tau_{lag}[s]$
1	$F(1.269, 10.156) = .991$ * $p = .365$	$F(2,16) = 2.056$ $p = .160$	$F(1.226, 9.807) = 1.211$ * $p = .311$
$\frac{1}{j\omega}$	$F(2,16) = .253$ $p = .780$	$F(1.038, 8.308) = .061$ * $p = .821$	$F(2,16) = .775$ $p = .477$
$\frac{1}{(j\omega)^2}$	$F(2,16) = 1.573$ $p = .238$	$F(2,16) = .364$ $p = .701$	$F(2,16) = 2.015$ $p = .166$

$H(\omega)$	$\tau_e[s]$	$\omega_c[Hz]$	$GX[Hz]$
1	$F(2,16) = .614$ $p = .554$	$F(2,16) = .797$ $p = .468$	$F(2,16) = .324$ $p = .728$
$\frac{1}{j\omega}$	$F(2,16) = .010$ $p = .990$	$F(2,16) = .068$ $p = .935$	$F(2,16) = .421$ $p = .664$
$\frac{1}{(j\omega)^2}$	$F(2,16) = .614$ $p = .553$	$F(1.261, 10.084) = 2.477$ * $p = .144$	$F(2,16) = .009$ $p = .991$

3.3. Test-retest reliability

3.3.1. Overview

To determine the reliability of the test results, the test-retest reliability has to be studied. The first part shows the test-retest results and a statistical analysis is performed in the second part.

3.3.2. Parameter estimation

Appendix C shows the mean estimated parameters, the crossover and cuttoff frequencies from nine subjects who did tests 1, 2 and 3. These values are in the same range of the values from Table 3.1.

3.3.3. Repeated-measures ANOVA

From the repeated-measures ANOVA's in Table 3.5 can be concluded that the estimated parameters $K[-]$, $\tau_{lead}[s]$, $\tau_{lead}[s]$ and $\tau_e[s]$ and crossover frequency $\omega_c[Hz]$ and cutoff frequency $GX[Hz]$ of the three tests do not significantly differ $p > .05$. This suggests that the test results are reliable. It should be highlighted that the p-values for the effective time delay $\tau_e[s]$ and crossover frequency $\omega_c[s]$ for the interaction with the integrator are extraordinary high.

4

Discussion

4.1. Overview

This study focused on a new method to find accurate performance measures of a mediolateral centre of mass(CoM)-controlled visual tracking task (VTT). During this task, subjects (n=21) were supposed to use mediolateral full-body displacement to track a target on a screen in three test conditions. In the first condition, the controlled element was a static gain, it was an integrator in the second condition and a double integrator in the third condition. The McRuer crossover model was used to describe the human frequency response. The crossover frequency $\omega_c[Hz]$ and the cutoff frequency $GX[Hz]$ were calculated. These values and the effective time delay $\tau_e[s]$ were the performance descriptors. In this chapter, the validity of the McRuer crossover model, the test protocol and the accuracy of the performance descriptors will be discussed.

4.2. The McRuer Crossover Model

The first subquestion of this study was *"Is the McRuer crossover model [3] able to describe the human frequency response while performing a balance-controlled VTT while interacting with a static gain /integrator /double integrator as the controlled element?"* This section discusses the human frequency response while performing a balance-controlled VTT. First, the time-domain behaviour and coherence will be discussed in general. Then, the human response in the frequency domain and the parameter estimation of the McRuer crossover model will be discussed for interacting with each controlled element separately.

4.2.1. General

Time domain

The results in the time domain (Figure 3.1) indicate that a human balance control system is able to accurately track a target during condition 1, the human balance control system reacts approximately the same during the three repetitive cycles of the trial. This can be confirmed by the error value that deviates around zero and the small deviation around the mean. These results implicate that the human frequency response $G(\omega)$ while interacting with a static gain can be considered time invariant [3].

A human balance control system appears to be able to track a target with an integrator-controlled tracker as well. However, the results indicate the tracking is less accurate according to the larger error deviation compared to that of condition 1. Also the deviation around the mean is larger compared to that of the static gain, which indicates that it is harder to track the target with an integrator-controlled target in a constant way.

From the bottom row of the figure it can be seen that the human balance control system appears to have great difficulty with accurately tracking the double integrator-controlled target. The deviations of CoM displacement $u[t]$ and displacement of the tracker $x[t]$ are large, meaning that the human balance control system reacts differently every repetitive cycle. The tracking error $e[t]$ is the largest of the three conditions, indicating that the differences between the tracker and target are large. However, the error is not constant.

Coherence

As explained in Section 3.1.2 the coherence is a measure for the linearity and the amount of noise at each frequency in the FRF. The higher the coherence, the more reliable the estimate of the transfer function. From the FRF's (Figures 3.2 and 3.3) it can be seen that the coherence decreases for increasing frequencies. This indicates that the subjects have increasing difficulty with tracking the target for increasing frequencies and the (measurement) noise takes prominence on the estimated frequency response.

The overall coherence of both the controlled element $H(\omega)$ and the human frequency response $G(\omega)$ of condition 1 and 2 is relatively high; that of condition 1 is slightly higher than condition 2. The coherence of condition 3 is low. This is mainly caused by the low linearity as can be seen by the greatly varying error signal in the time domain. So, as was expected from the time domain results, the coherence suggests that the subjects have less difficulty with condition 1 or 2 compared to condition 3. *Moreover, the overall coherence of condition 3 is too low so no valid conclusions can be drawn from the FRF. Therefore, the data of condition 3 will not be taken into discussion.*

Because of the decreasing coherence for increasing frequency, the human balance control system can be regarded as a low-pass filter [18], with a different bandwidth for interacting with each controlled element. This can be seen more clearly in the closed-loop FRF (Figure 3.4), where the performance of the human balance control system is high at first and drops at a certain frequency, which is the crossover frequency.

In the next sections, the coherence of the human frequency response $G(\omega)$ for condition 1 and 2 will be discussed as well as the crossover frequency as performance measure.

4.2.2. Condition 1

Frequency domain

Regardless of the decreasing coherence for increasing frequencies, the estimated controlled element averaged over all subjects (Figure 3.2) shows pure static gain response; the gain is constant and the phase is $0\,\mathrm{deg}$ for all frequencies.

The estimated human frequency response averaged over all subjects shows that the human balance control system $G(\omega)$ appears to be a delayed and amplified integrator as expected because the slope of the gain is approximately -1 and the phase starts more or less at $-90\,\mathrm{deg}$. The time delay is caused by the physiological delays of the human body. The ratio of the COM displacement with respect to the displacement of the target and tracker on the display causes the amplification. This will differ with the screen size used to project the application, but will have no effect on the further results, only on the value of the gain.

Crossover model

For the human frequency response to be a (delayed and amplified) integrator, values of time constants $\tau_{lead} = 0s$ and $\tau_{lag} >> 0s$ are expected according to the McRuer crossover model [3]. The values of the mean and standard deviation calculated over 21 subjects of $\tau_{lead} = 0.11(0.07)s$ and $\tau_{lag} = 3.25(2.34)s$. These values indicate that the human frequency response is a (delayed and amplified) integrator and therefore behaves like a lag-lead equalizer [3].

The mean value and standard deviation of the effective time delay $\tau_e = 0.33(0.13)s$ corresponds with the values stated by Stassen and McRuer [13], [3]. This value is on the lower side of the range stated by Stassen, which suggests that the complexity of the test while interacting with a static gain is rather low.

In this test condition, the open-loop frequency response around the crossover frequency $\omega_c[Hz]$ is an integrator as can be concluded from Figure 3.4. The value of the crossover frequency $\omega_c = 0.61(0.13)Hz$, which is slightly lower than the $0.80 - 0.95Hz$-range that was stated by McRuer [3]. The frequency range from zero to ω_c is the bandwidth of the subjects, which shows until what frequency the subjects were able to track the target. A lower crossover frequency than in McRuer's study can be assigned to the fact that McRuer used trained fighter pilots were able to track the target more accurately. Also, the tracker in McRuer's study was controlled with a joystick, wrist movements probably take less effort compared to full body displacement. However, the difference between this condition's crossover frequency and that of McRuer's study are not significant.

The value of $GX = 1.24(0.54)Hz$. This is comparable with the value that is measured in MELBA (Table 1.2) [1].

4.2.3. Condition 2

Frequency domain

The estimated controlled element $G(\omega)$ averaged over all subjects responds like an integrator for the lower frequencies. For increasing frequency, the coherence is approximately zero so the estimate deflects from the transfer function of the measured data. The slope of the gain is -1 and the phase is equal to $-90\,\mathrm{deg}$.

The human frequency response averaged over all subjects (Figure 3.2) shows that the averaged human balance control system appears to respond like a delayed static gain for the lower frequencies with a higher coherence, because the gain is constant and the phase starts at approximately zero.

Crossover model

For the human frequency response to be a (delayed and amplified) static gain, values of $\tau_{lead} = 0s$ and $\tau_{lag} = 0s$ are expected. The values of the mean and standard deviation calculated over 21 subjects of $\tau_{lead} = 0.20(0.29)s$ and $\tau_{lag} = 0.35(0.22)s$. These values indicate that the human balance control system indeed responds like a delayed and amplified integrator in this test and therefore behaves as a high-frequency lead equalizer [3].

The effective time delay of condition 2 $\tau_e = 0.30(0.23)s$. It is lower than the value of $\tau_e[s]$ of condition 1. This is notable, since the value of $\tau_e[s]$ of condition 2 was higher compared to that of condition 1 as stated by McRuer (Table 1.2). The reason for this shorter time delay could be that subjects were more focused during this condition, because the task was more difficult than condition 1. Nevertheless, the standard deviation of $\tau_e[s]$ of the second condition is much higher compared to that of the first condition. Therefore, the values of $\tau_e[s]$ do not significantly differ from each other (Table 1.2). This might be the case because the visual information did not get more difficult. The subjects had to process the same visual input as in condition 1. The values are still in the same range as stated by McRuer and Stassen [3], [13].

The calculated value of the crossover frequency of condition 2 $\omega_c = 0.20(0.06)Hz$. This value is smaller than the crossover frequency of condition 1, this indicates that the performance is lower for this condition; the subjects were able to track until a lower frequency than in condition 1. The values were also lower than the value stated by McRuer, however this difference is not significant.

The value of $GX[Hz] = 0.39(0.09)$. Comparing this value is neither possible with MELBA results nor with the crossover frequency ω_c, since the values of the crossover frequency and GX are not correlated for condition 2.

Summarizing, the human balance control system appears to respond like an integrator during condition 1 and like a static gain during condition 2. However, the values of the effective time delay is lower for the more complex condition instead of higher like the values of McRuer, although, these differences are not significant. As well as in the crossover model, the value of the crossover frequency $\omega c[Hz]$ of condition 1 is the highest and lowest for condition 3, suggesting that the McRuer crossover model might be applicable to balance-controlled visual tracking tasks. This indicates that this model can be applied to further analysis.

4.3. Test-Retest reliability

The second subquestion of the study was *"Is the protocol test-retest reliable?"* If this were the case, the results should not significantly differ after repeating the test or a learning effect should be clearly visible. In other words, for good reproducibility the subjects should react the same way every time they perform in the test. Inaccuracy during the test protocol or measurement noise could lead to a decreased test-retest ability.

To study the test-retest ability of the protocol, it was performed three times with two days and a month in between respectively (n=9), resulting in sets of three times each parameter. The sets were analysed by a repeated-measures ANOVA. The results (Table 3.5) indicate that the differences of the values within a set are not significant, because the p-values were much higher than 0.05. This means that sets of parameters are not significantly different. However, this subject group is too small, so a larger group of subjects has to be assessed to be able to draw valid conclusions.

4.4. Accuracy

Finally, the question *"Which parameter, the effective time delay $\tau_e[s]$, the crossover frequency $\omega_c[Hz]$ or the cutoff frequency $GX[Hz]$, in what condition, might be an accurate performance measure?"* is discussed. For the purpose of diagnostics, the level of a test should not be too low, because then all subjects will be able to perform excellently and ceiling effects will occur. If a test then might not notice impairment, this is called a false negative diagnosis. This also yields when the level is too high and no one will be able to perform well, whereby too many people might be diagnosed, which is called a false positive diagnosis. Therefore, the level of a test should be somewhere in between. The performance measures should be accurate, so the standard deviation should be low. Moreover, it is also of importance to keep the comfort of the subject in mind.

First, according to the crossover frequencies, it can be concluded that the subjects were able to track the target to a higher frequency during condition 1 than condition 2. However, the test did not show ceiling effects, even with healthy subjects. Therefore it is unlikely that testing a subject at risk of falling would show ceiling effects, because it is expected that their crossover frequency will be lower. This shows potential of this protocol as a balance assessment method.

The protocol took 3x45 seconds for each condition. The subjects were tested for a broad range of frequencies between 0 and 3 Hz. If the crossover frequencies of people at risk are known, this frequency range can be specified and the protocol can be shortened. The measured values of the crossover frequency $\omega_c[Hz]$ indicate that $\omega_c[Hz]$ of condition 1 is more than two times higher than that of condition 2. With a higher frequency-range is it possible to have a shorter test protocol. This is beneficial for the comfort of the subject.

The ratios between the mean values and standard deviations of $\tau_e[s]$, $\omega_c[Hz]$ and $GX[Hz]$ (Table 3.1) of condition 1 and 2 are evaluated to see what values are approximately similar for all healthy subjects. Looking at condition 1, the deviations of $\tau_e[s]$ and $GX[Hz]$ are relatively high. That of $\omega_c[Hz]$ is generally lower, indicating that this parameter might be a good measure for condition 1.

On the contrary, $GX[Hz]$ of condition 2 has the lowest deviation ratio. The ration of τ_e is extremely high and therefore seems to be less suitable for the use as measure in condition 2. However, maybe is this the case because this parameter is extremely sensitive, which would be beneficial for the diagnosis of individuals. This can only be verified by testing and comparing more specific subject groups.

The significance values (Table 3.5) of condition 2 are high compared to those of condition 1, indicating a high reliability of these values. When interacting with the controlled element as integrator, condition 2, the human balance control system reacts like a static delayed gain. The time constants $\tau_{lead}[s]$ and $\tau_{lag}[s]$ are therefore approximately zero, so a simpler model might be usable to study the human frequency response.

Summarizing, The crossover frequency $\omega_c[Hz]$ and the cutoff frequency $GX[Hz]$, of both the static gain and integrator conditions have their advantages and disadvantages on behalf of the early detection of people at risk of falling.

4.5. Recommendations

Further analysis should explore which performance measure is the most accurate and sensitive. It is important to study which condition is the best in distinguishing between patient groups or between individual subjects. Therefore, the two test conditions should be repeated with a larger subject group, as well as a subject group with known impaired balance.

5

Conclusion

The goal of this study was to find out whether a mediolateral centre of mass-controlled visual tracking task, provides accurate performance measures. First the human balance control system was assessed during three visual feedback conditions and the frequency responses were compared thereafter.

The results demonstrated that the McRuer crossover model [3] is a powerful tool to describe human frequency response during balance-controlled visual tracking tasks and the test protocol has a high test-retest reliability. The results of test condition 3 were not valid.

The crossover frequency $\omega_c[Hz]$ and the cutoff frequency $GX[Hz]$, of both the static gain and integrator conditions have their advantages and disadvantages on behalf of the early detection of people at risk of falling. However, the two test conditions should be repeated with a larger subject group, as well as a subject group with known impaired balance, to find out which performance measure is the most accurate and sensitive.

Bibliography

[1] L. E. C. Lizama, M. Pijnappels, N. P. Reeves, S. M. Verschueren, and J. H. van Dieën, *Frequency domain mediolateral balance assessment using a center of pressure tracking task,* Journal of biomechanics **46**, 2831 (2013).

[2] L. E. C. Lizama, M. Pijnappels, G. H. Faber, P. N. Reeves, S. M. Verschueren, and J. H. van Dieen, *Age effects on mediolateral balance control,* PloS one **9**, e110757 (2014).

[3] D. T. McRuer and H. R. Jex, *A review of quasi-linear pilot models,* Human Factors in Electronics, IEEE Transactions on , 231 (1967).

[4] J. Browne, N. O'Hare, G. O'Hare, A. Finn, and J. Colin, *Clinical assessment of the quantitative posturography system,* Physiotherapy **88**, 217 (2002).

[5] K. Berg, *Measuring balance in the elderly: preliminary development of an instrument,* Physiotherapy Canada **41**, 304 (1989).

[6] D. Engelhart, J. H. Pasma, A. C. Schouten, C. G. Meskers, A. B. Maier, T. Mergner, and H. van der Kooij, *Impaired standing balance in elderly: A new engineering method helps to unravel causes and effects,* Journal of the American Medical Directors Association **15**, 227 (2014).

[7] A. F. Ambrose, G. Paul, and J. M. Hausdorff, *Risk factors for falls among older adults: a review of the literature,* Maturitas **75**, 51 (2013).

[8] D. Sturnieks, R. St George, and S. Lord, *Balance disorders in the elderly,* Neurophysiologie Clinique/Clinical Neurophysiology **38**, 467 (2008).

[9] M. E. Tinetti, C. S. Williams, and T. M. Gill, *Dizziness among older adults: a possible geriatric syndrome,* Annals of Internal Medicine **132**, 337 (2000).

[10] S. G. Brauer, Y. R. Burns, and P. Galley, *A prospective study of laboratory and clinical measures of postural stability to predict community-dwelling fallers,* The Journals of Gerontology Series A: Biological Sciences and Medical Sciences **55**, M469 (2000).

[11] B. E. Maki, P. J. Holliday, and A. K. Topper, *A prospective study of postural balance and risk of falling in an ambulatory and independent elderly population,* Journal of Gerontology **49**, M72 (1994).

[12] M. J. Hilliard, K. M. Martinez, I. Janssen, B. Edwards, M.-L. Mille, Y. Zhang, and M. W. Rogers, *Lateral balance factors predict future falls in community-living older adults,* Archives of physical medicine and rehabilitation **89**, 1708 (2008).

[13] H. Stassen, *Mens-machine-systemen: regel-, stuur-en bewakingstaken,* JA Michon, E. GJ. Eijkman & LFW de Klerk (Eds.,). Handboek der Psychonomie. Deventer: Van Loghum Slaterus (1976).

[14] N. Moray, *Ergonomics: major writings* (Psychology Press, 2005).

[15] J. T. Bingham, J. T. Choi, and L. H. Ting, *Stability in a frontal plane model of balance requires coupled changes to postural configuration and neural feedback control,* Journal of neurophysiology **106**, 437 (2011).

[16] S. M. Henry, J. Fung, and F. B. Horak, *Effect of stance width on multidirectional postural responses,* Journal of Neurophysiology **85**, 559 (2001).

[17] A. Field, *Discovering statistics using SPSS* (Sage publications, 2009).

[18] A. D. Kuo, *An optimal state estimation model of sensory integration in human postural balance,* Journal of Neural Engineering **2**, S235 (2005).

A

D-Flow Application

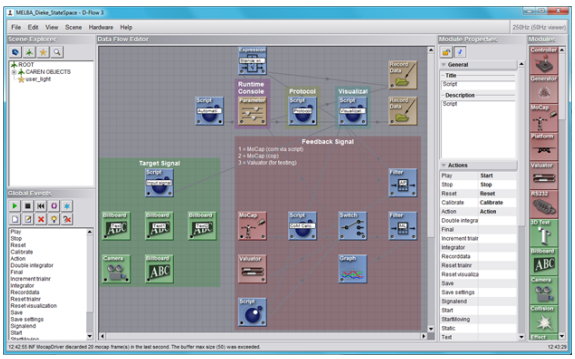
A.1. Introduction

The application that was designed for this study was programmed in D-Flow, by MotekForce Link. According to the corporate website D-flow is a control software suite that provides real-time data streams between many types of integrated hardware. In this study, the software enabled controlling a screen projection with location data derived from a motion capture system. This appendix illustrates how the application was composed. First, to give an overview of the application, its interface is shown. Then, the different components of the application are clarified.

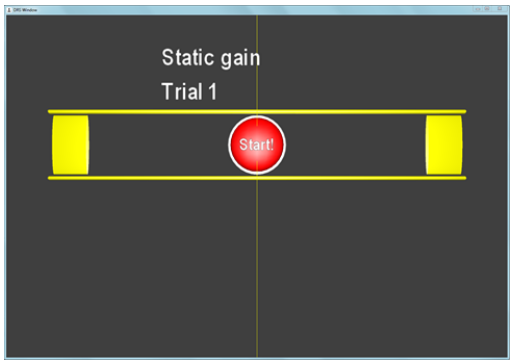
A.2. Interface Application

The D-Flow software mainly consists of the main window and the DRS window. These are shown in Figures A.1a and A.1b. The DRS window displays the test. This window is projected on a screen so the subject sees it.

In the centre of the main window, the Data Flow Editor is shown. The application is composed of modules, represented by blocks in the centre of the Data Flow Editor. A module is a preprogrammed part with a specific task that can be adjusted according to the requirements of the user. Examples of modules are MoCap, which connects with the motion capture system; Expression, which enables performing a simple calculation on the data stream; and Billboard, which displays custom text in the DRS window when activated. The Script module allows programming, which gives more freedom processing the data. The modules are connected by arrows, giving a visual representation of the data stream. The modules can be (de)activated by broadcasting an event. This is convenient if a certain module should start/stop after a pre-set time or when a Script module has ”finished”. The modules are grouped according to their function in the application. These will be clarified in the sections below.

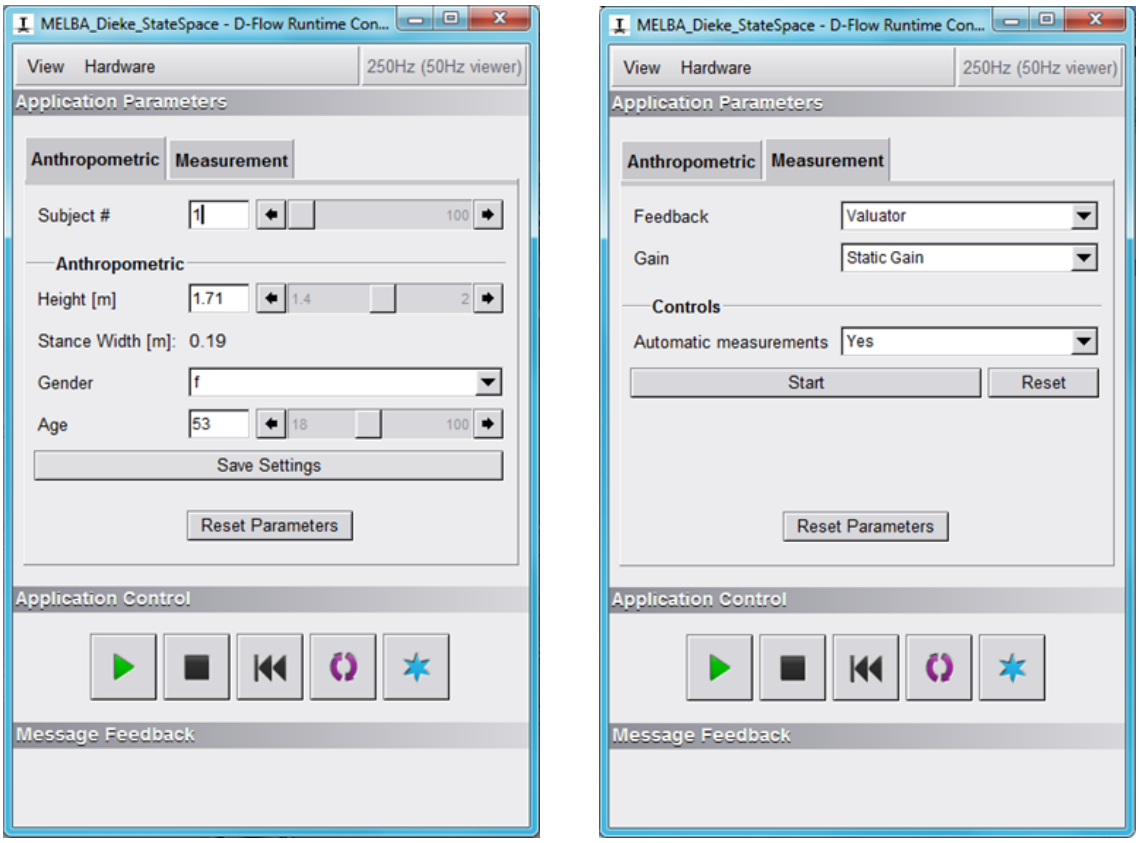


(a) The main interface



(b) The DRS window

Figure A.1: The application



(a) The anthropometric tab

(b) The measurement tab

Figure A.2: The Runtime Console

Runtime Console

The module Runtime Console is used to control the test. The first tab, shown in Figure A.2a is used to save the anthropometric characteristics of a subject. After clicking save settings, the settings will be saved to a text-file. After inserting the subject's length, the supposed stance width is automatically calculated and displayed.

In the measurement tab A.2b the settings for the target signal, how the tracker is controlled, which condition will be tested and whether the protocol should automatically continue can be adjusted. These settings are connected to switch modules and events in the application.

After adjusting the settings and before commencing the test, the application should be reset by hitting the stop and reset buttons of the Application Control. Then the measurement can be started by clicking on the start button. The protocol runs fully automated (if automatic measurements is set to 'yes') after clicking the start button in the Runtime Console.

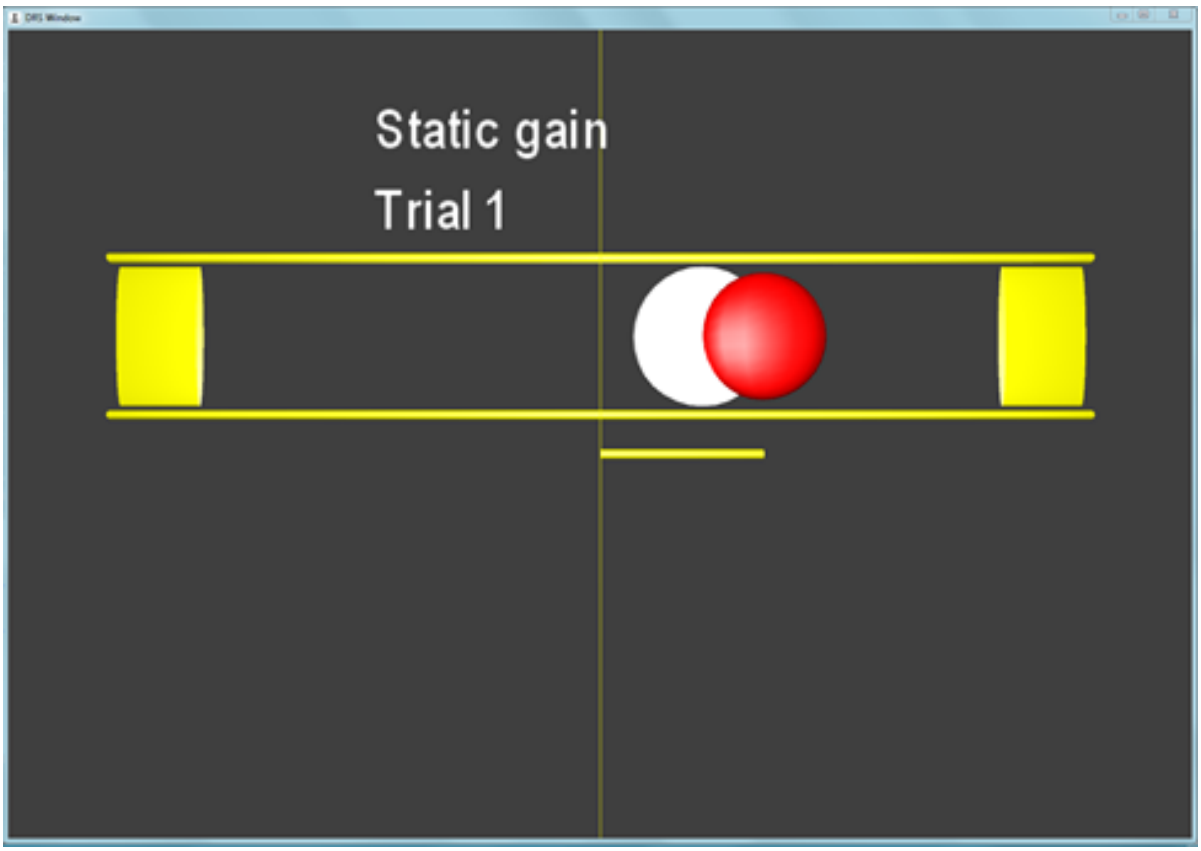


Figure A.3: The DRS window during a trial

Protocol

The protocol describes which actions should be taken in what order and timing during one test. This also involves controlling the hardware. After starting a trial, ”3, 2, 1, Start” is displayed and the target will be controlled by a produced signal. The first 10 seconds, the target does not move and the subject is able to practice displacing the tracker. Then the data recording starts and the amplitude of the multi sine controlling the target increases from 0 to normal in 5 s so that the participant gets used to the tracker’s reaction to COM movement and tracking the target. The target will continue to move for 30 seconds, shown in Figure A.3. Depending on the intial settings, a new trial will start either after clicking start or a by an automatically broadcasted start event.

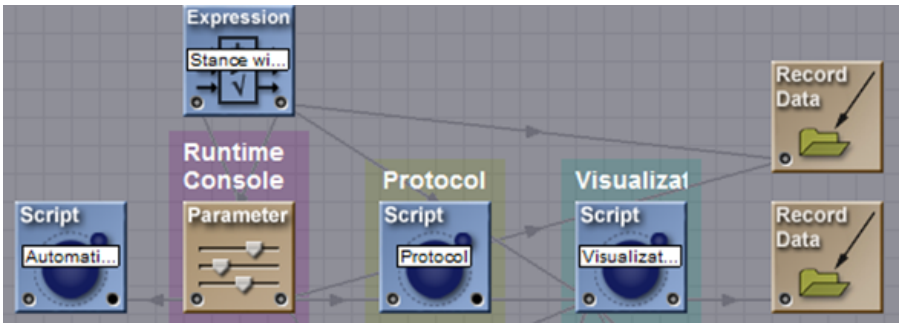
The application automatically changes the condition after four trials, controlled by the protocol Script module which can be seen in Figure A.4a. And it is not possible to start a trial without resetting the application as described above if the protocol has finished.

Target signal

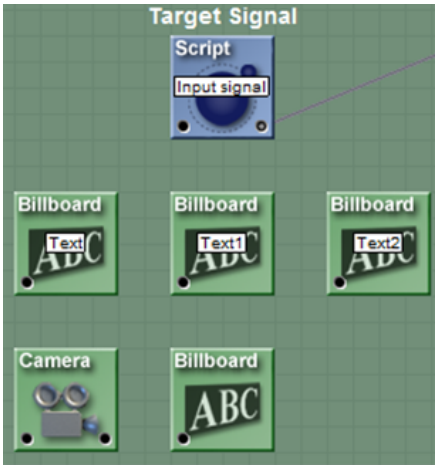
One can see the group called ”Target signal” in Figure A.4b from which the signal that controls the target is generated. The signal is a multisine containing the frequencies 0.1, 0.2, 0.3, 0.5, 0.7, 1.0, 1.4, 2.0, and 3.0 Hz with descending amplitudes. The random phase shifts are generated again for each trial so each target signal contains three unique, identical cycles of 10 seconds.

Feedback signal

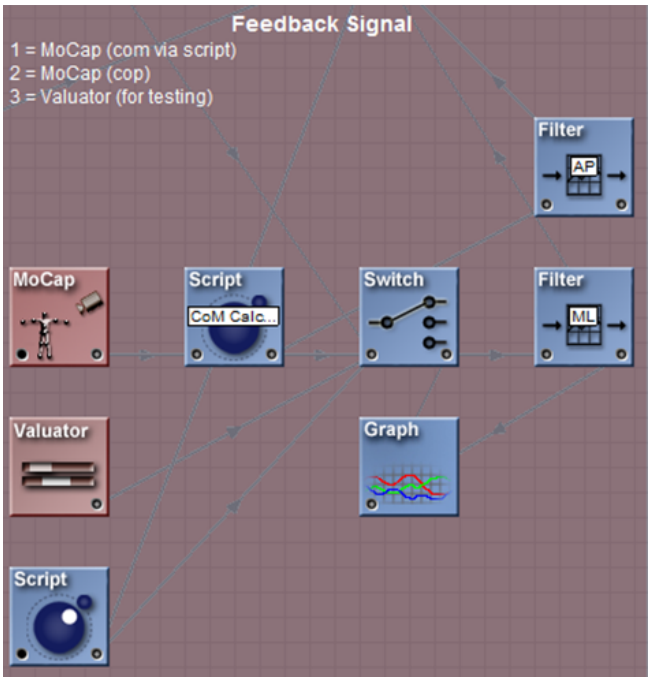
The tracker is controlled from the ”Feedback signal” group as shown in Figure A.4c. The source of this signal; motion capture, valuator data or a predefined multisine, can be set in the Runtime Console. The x-, y- and z-location data of the three markers, recorded by the motion capture system, are retrieved by the MoCap module. Only the x-location data is used to calculate the mediolateral displacement of the CoM of the subject. The data that is used for controlling the tracker is filtered before it is used to



(a) The Runtime Console, Protocol and Visualization module groups



(b) The target module group



(c) The tracker module group

Figure A.4: The module groups

be displayed.

Visualization

In Figure A.4a, the Visualization module is shown. From there, the DRS window is controlled. First, the objects are created. Then, when the protocol starts, the horizontal locations of the target and tracker will be calculated with the target and tracker signals. The signal of the target is used directly. The signal of the tracker is transformed with a state space calculation that depends on the test condition. The gain that is used, depends on the source of the signal.

Data recording

The data streams are real-time recorded with the Record module, shown in Figure A.4a. Each data sample is saved in a text-file on a new line; the different signals are divided by tabs resulting in columns.

B

Frequency response subjects

Subject 1

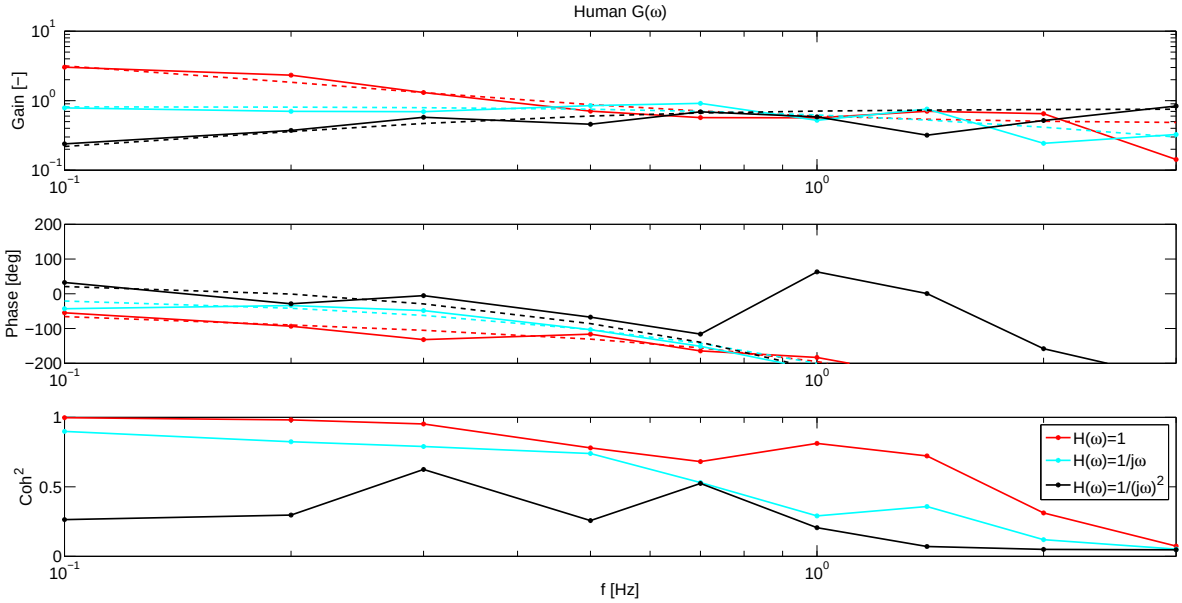


Figure B.1: Magnitude, phase and coherence estimated from spectral densities (—) and crossover model(- -)

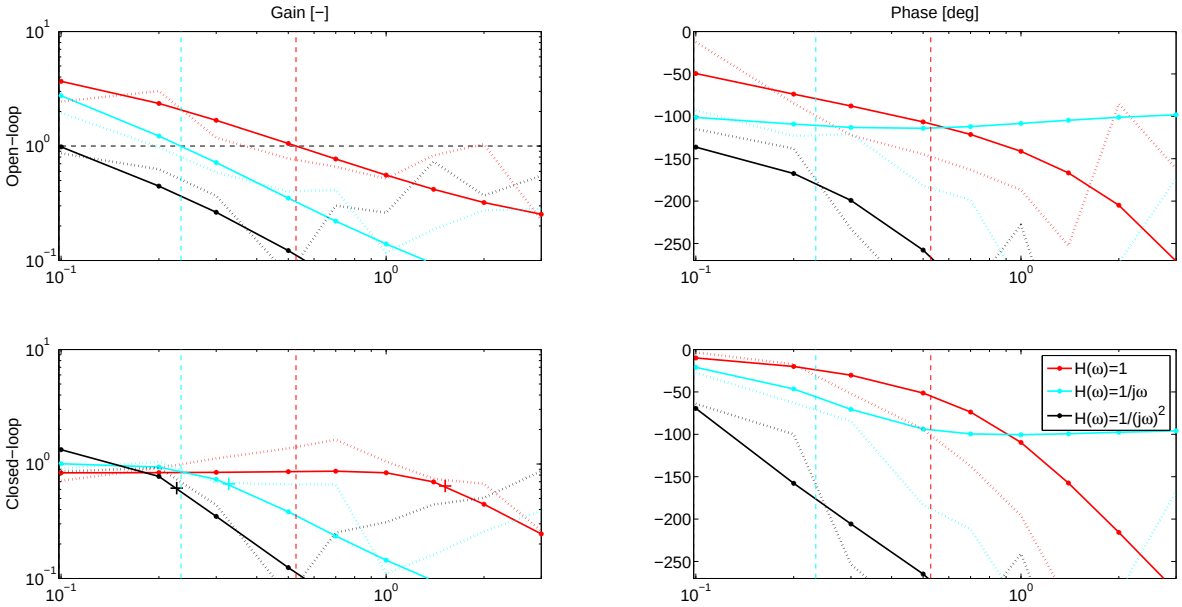


Figure B.2: Crossover frequency (- -) and cutoff frequency (+)

Subject 2

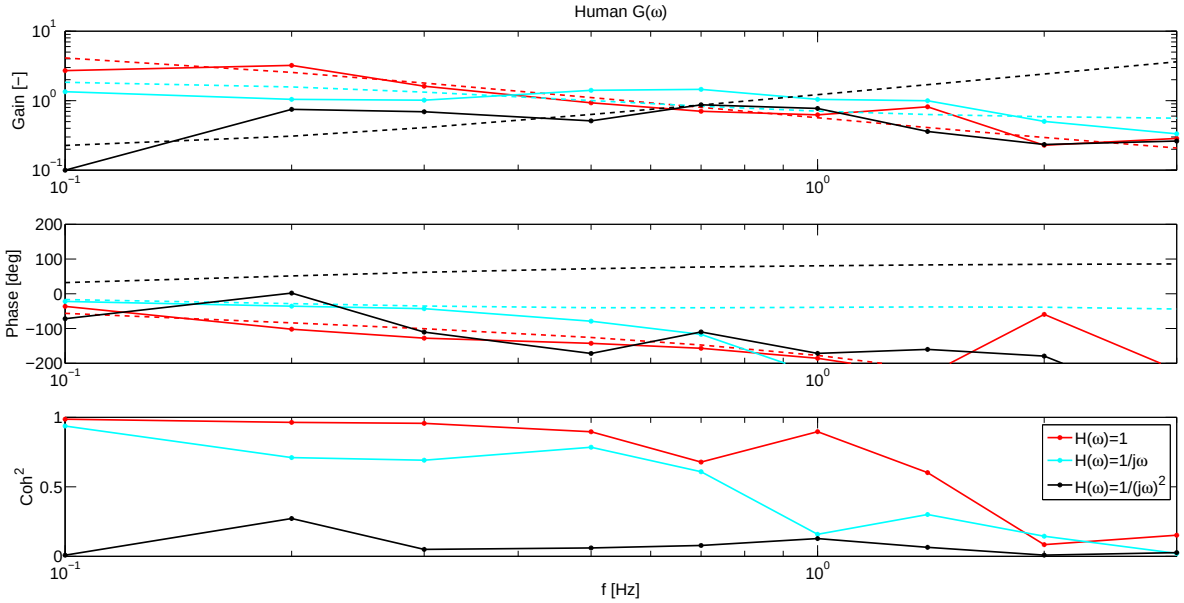


Figure B.3: Magnitude, phase and coherence estimated from spectral densities (—) and crossover model(- -)

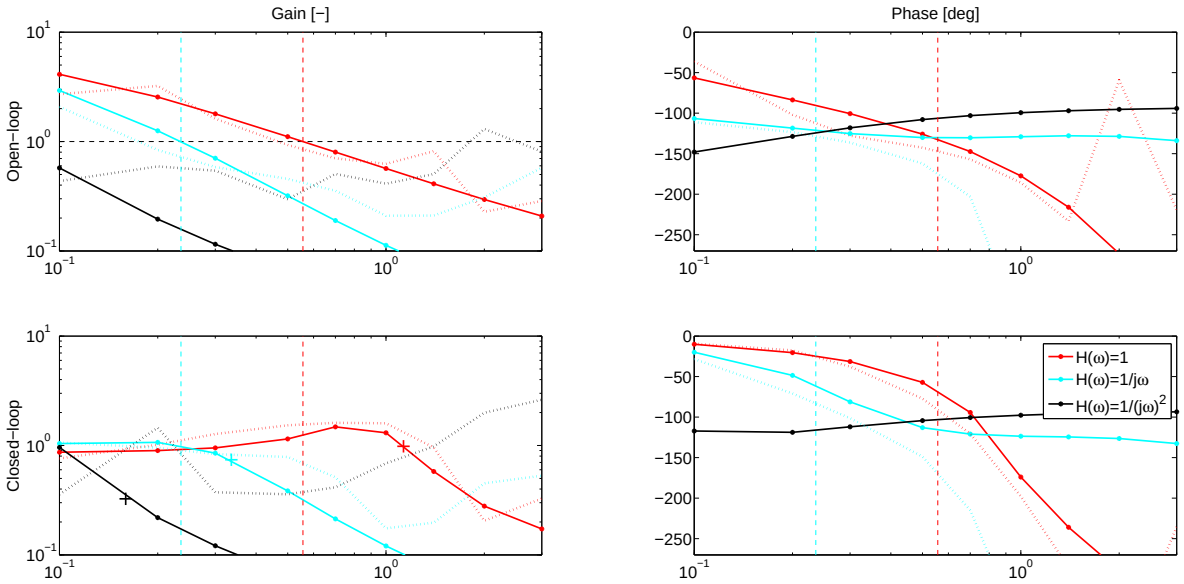


Figure B.4: Crossover frequency (- -) and cutoff frequency (+)

Subject 3

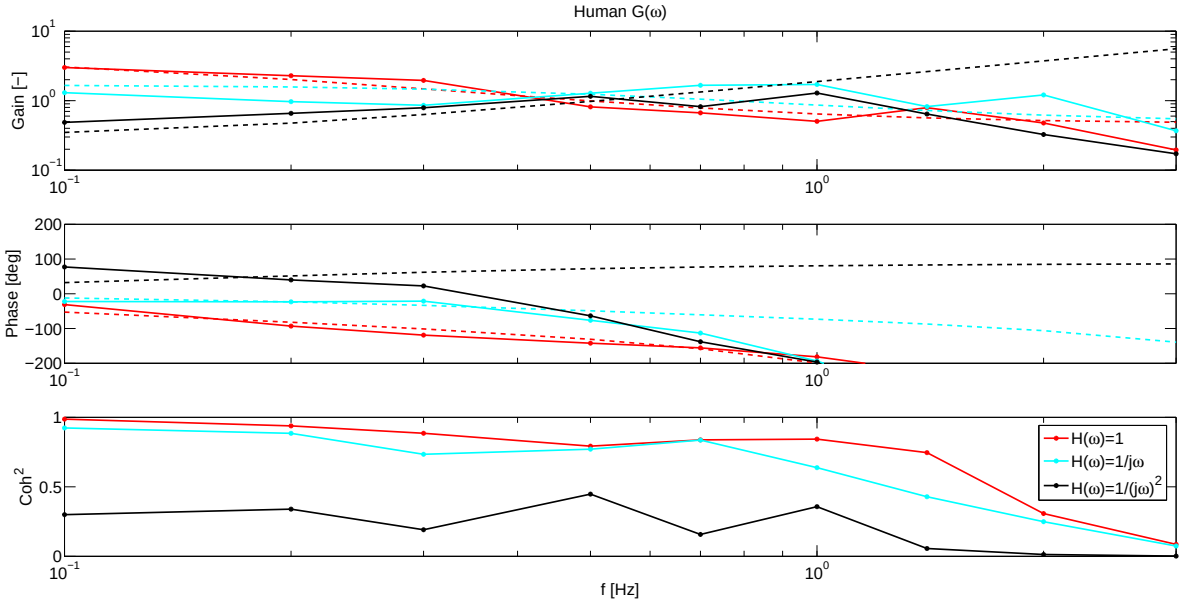


Figure B.5: Magnitude, phase and coherence estimated from spectral densities (—) and crossover model(- -)

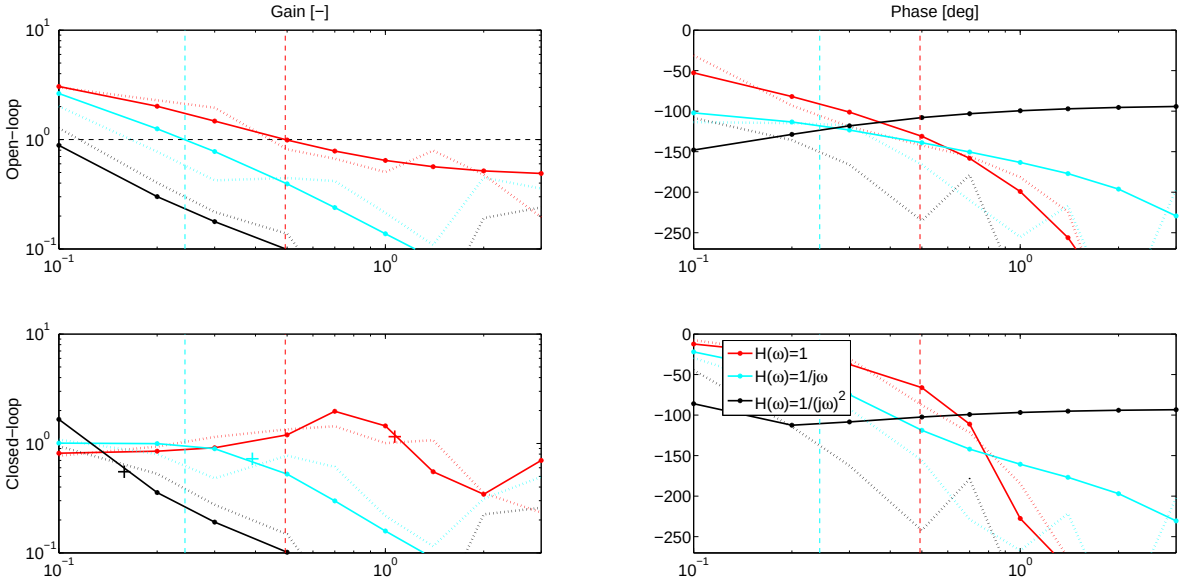


Figure B.6: Crossover frequency (- -) and cutoff frequency (+)

Subject 4

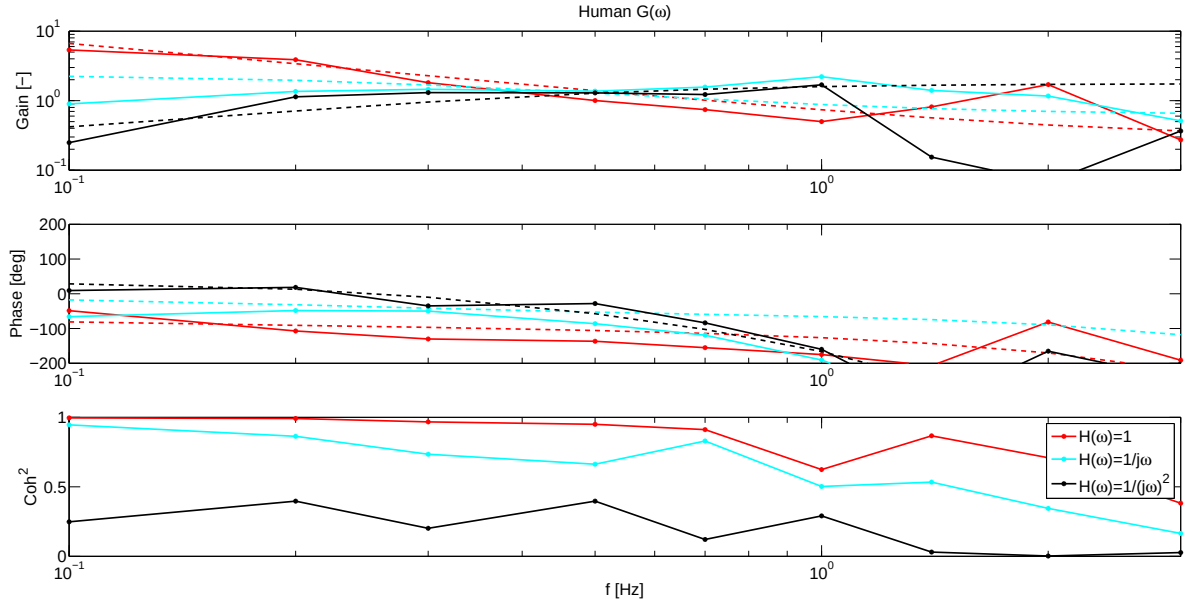


Figure B.7: Magnitude, phase and coherence estimated from spectral densities (—) and crossover model(- -)

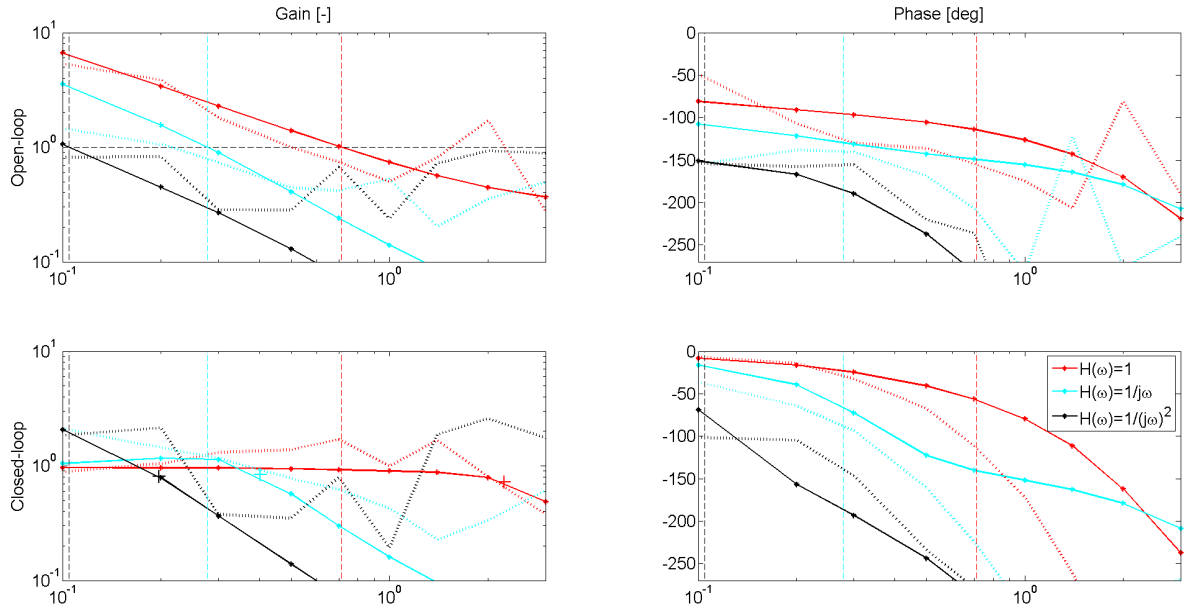


Figure B.8: Crossover frequency (- -) and cutoff frequency (+)

Subject 5

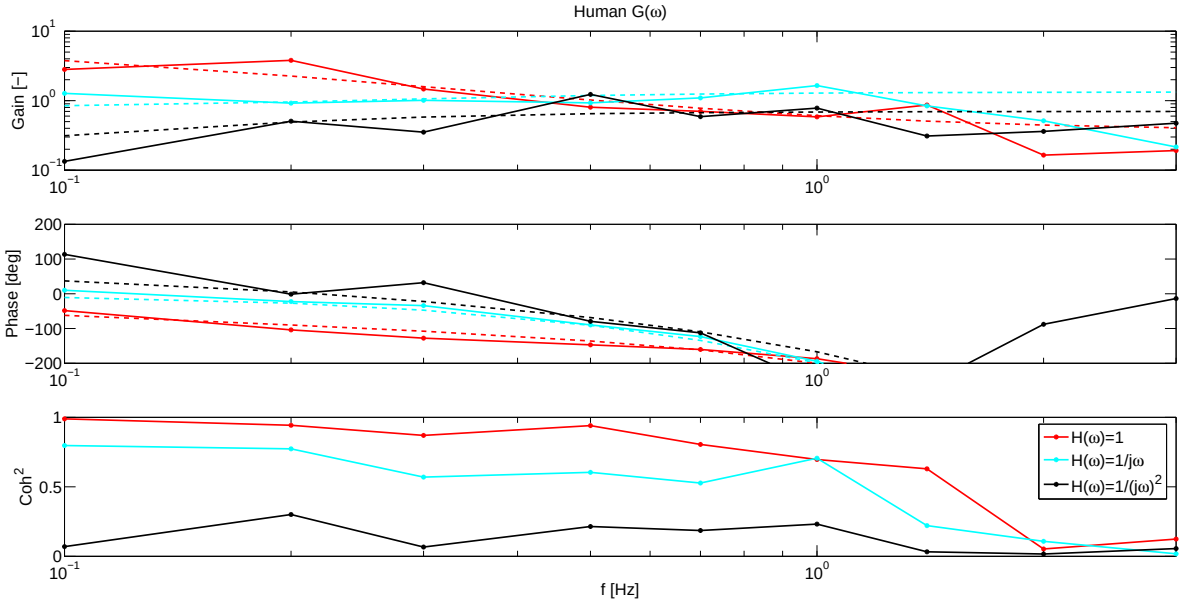


Figure B.9: Magnitude, phase and coherence estimated from spectral densities (—) and crossover model(- -)

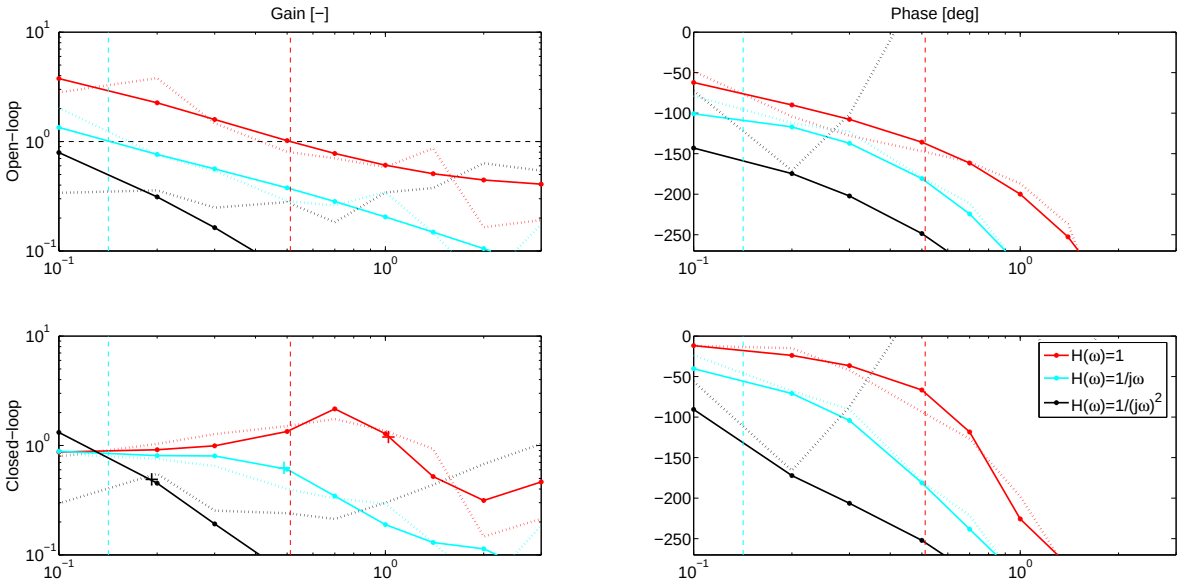


Figure B.10: Crossover frequency (- -) and cutoff frequency (+)

Subject 6

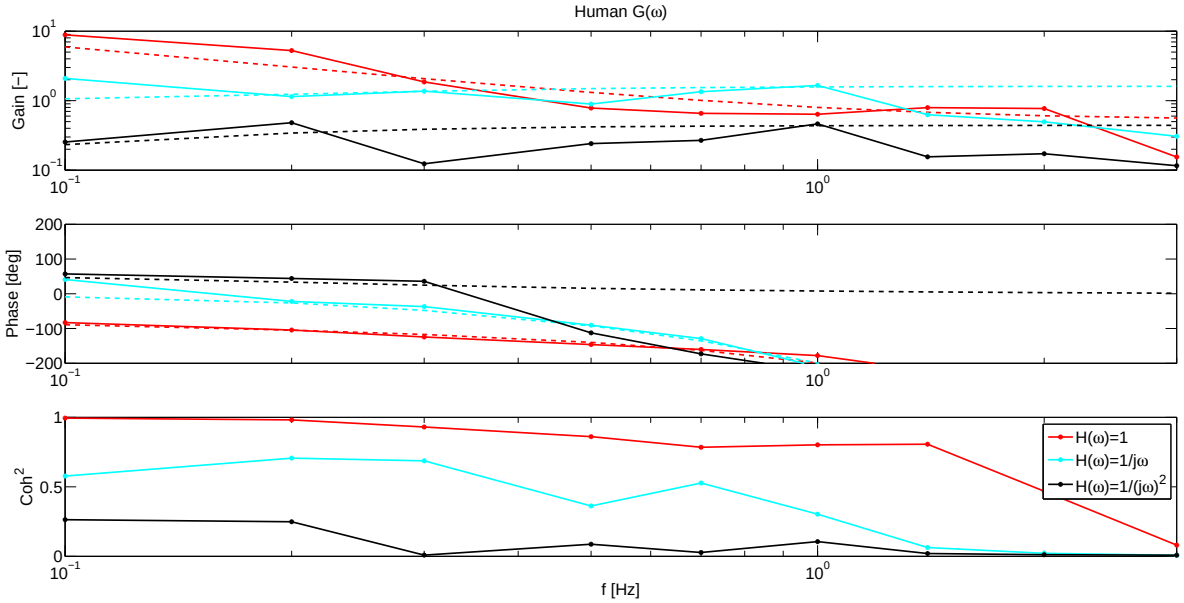


Figure B.11: Magnitude, phase and coherence estimated from spectral densities (—) and crossover model(- -)

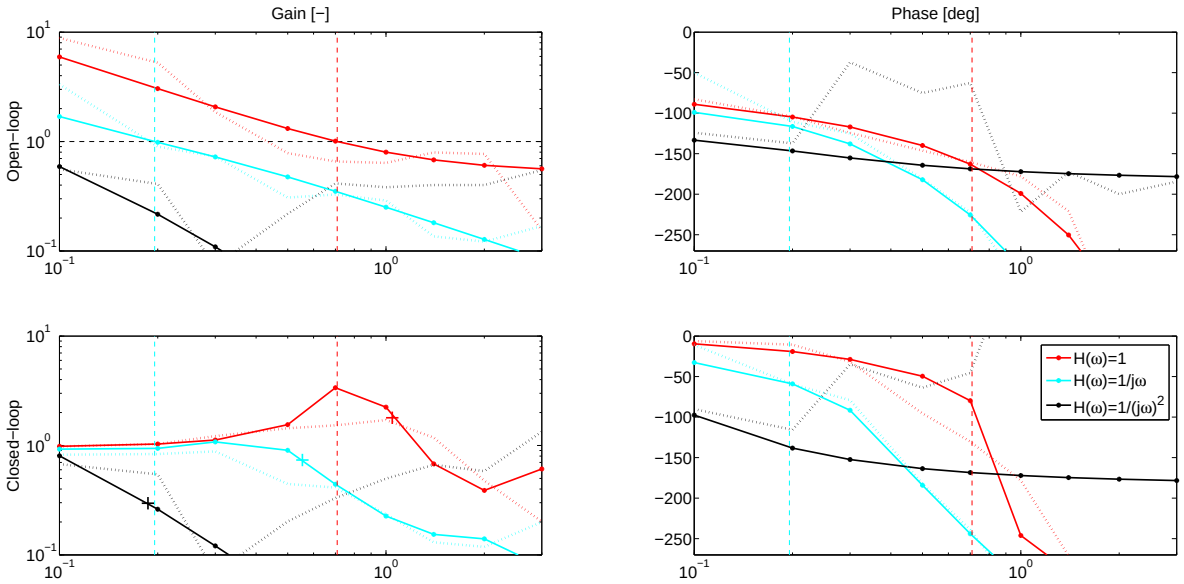


Figure B.12: Crossover frequency (- -) and cutoff frequency (+)

Subject 7

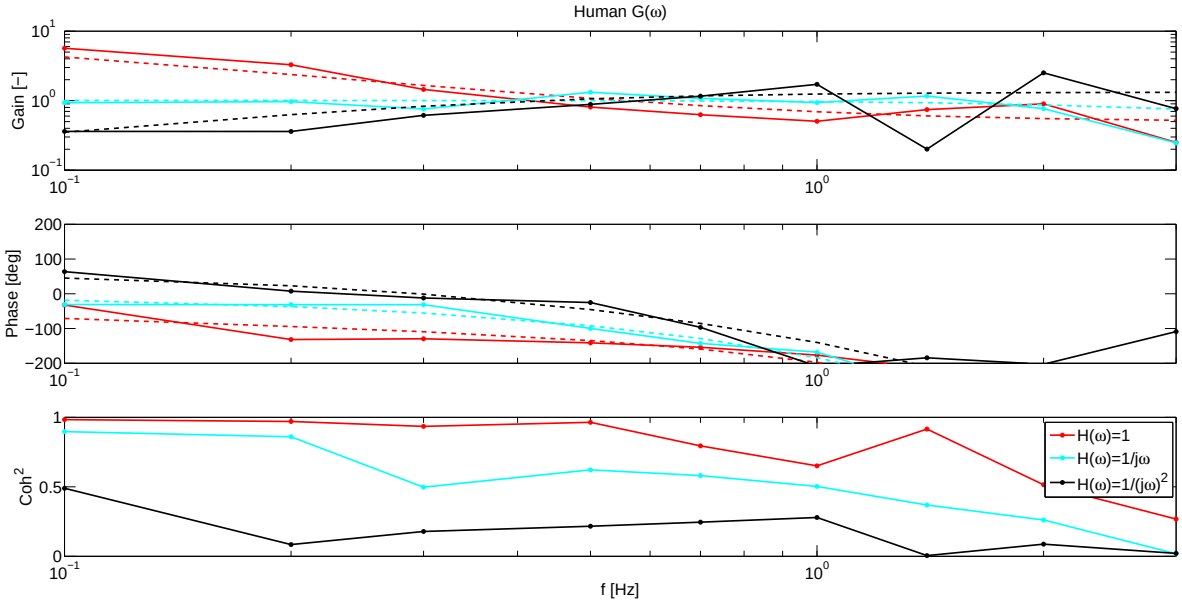


Figure B.13: Magnitude, phase and coherence estimated from spectral densities (—) and crossover model(- -)

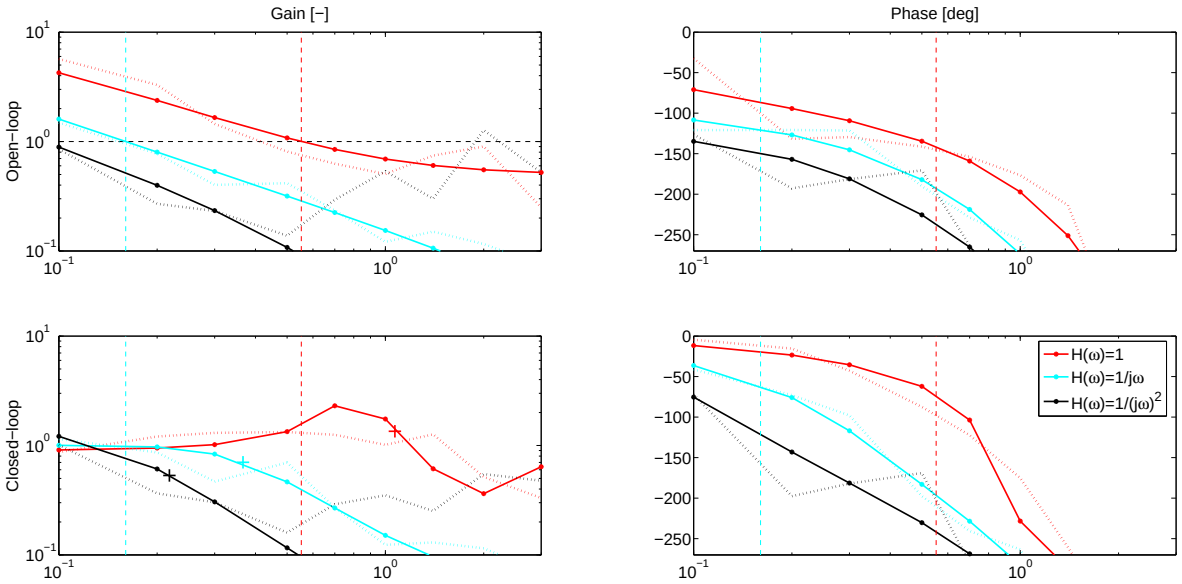


Figure B.14: Crossover frequency (- -) and cutoff frequency (+)

Subject 8

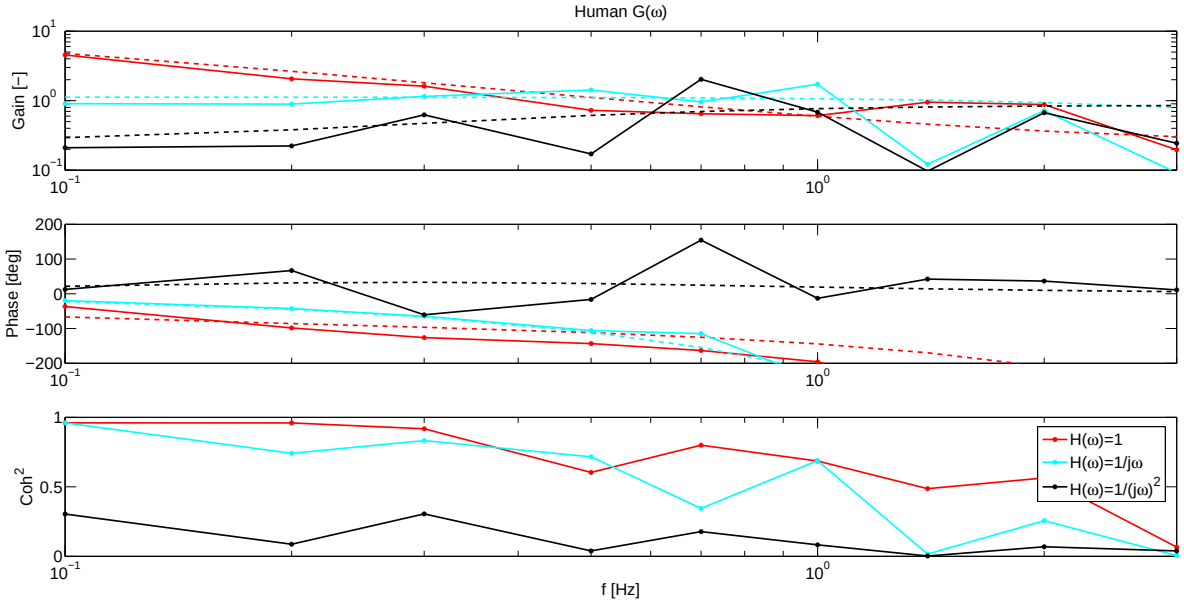


Figure B.15: Magnitude, phase and coherence estimated from spectral densities (—) and crossover model(- -)

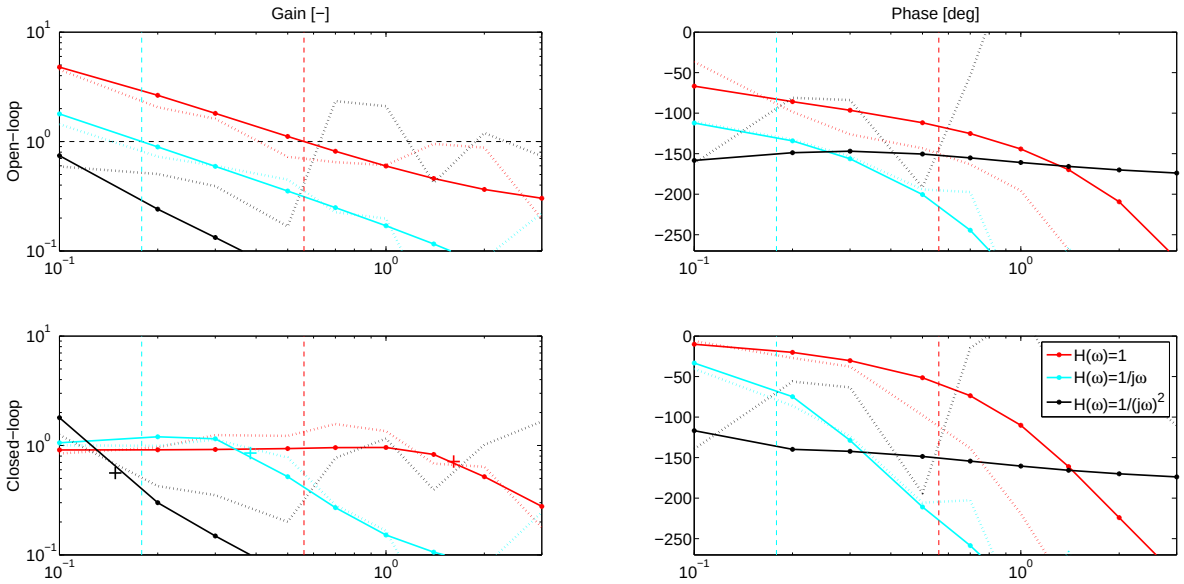


Figure B.16: Crossover frequency (- -) and cutoff frequency (+)

Subject 9

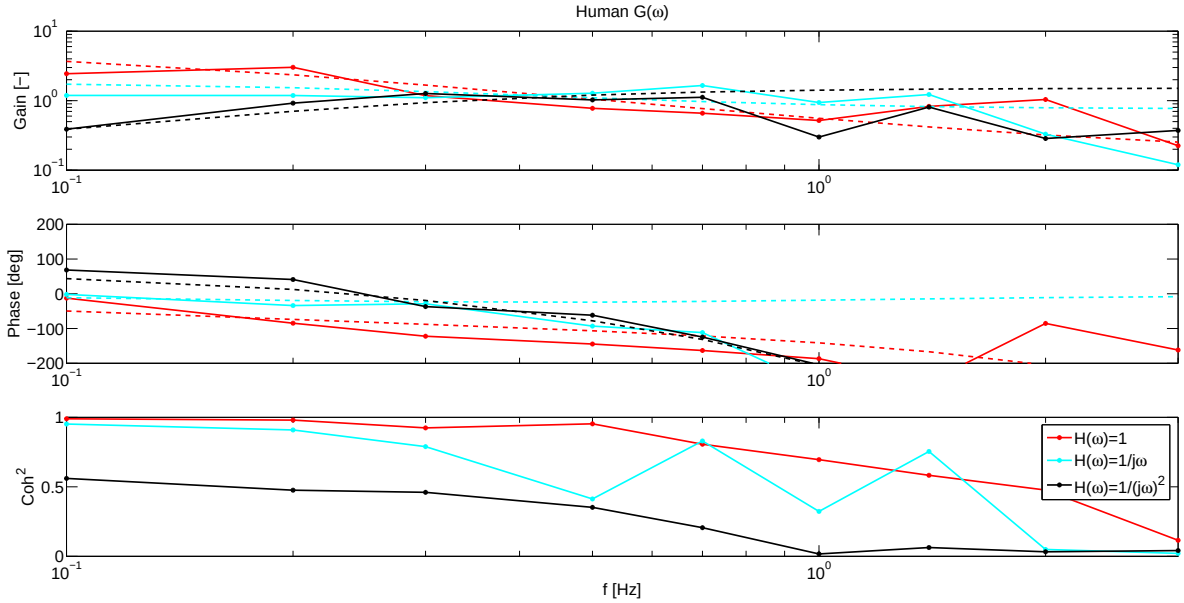


Figure B.17: Magnitude, phase and coherence estimated from spectral densities (—) and crossover model(- -)

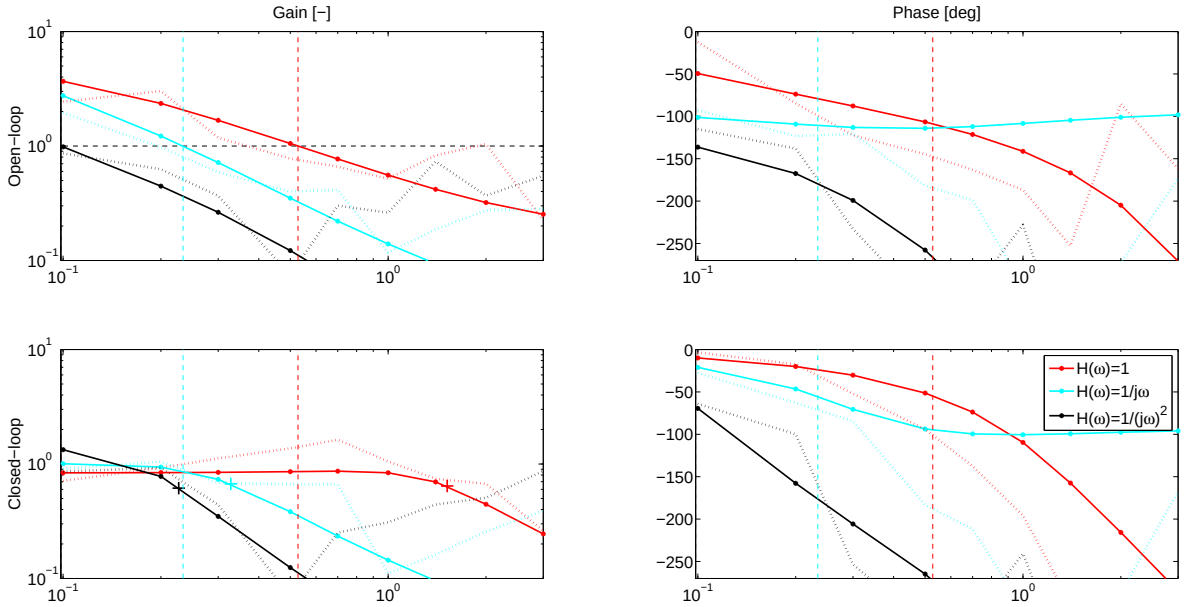


Figure B.18: Crossover frequency (- -) and cutoff frequency (+)

Subject 10

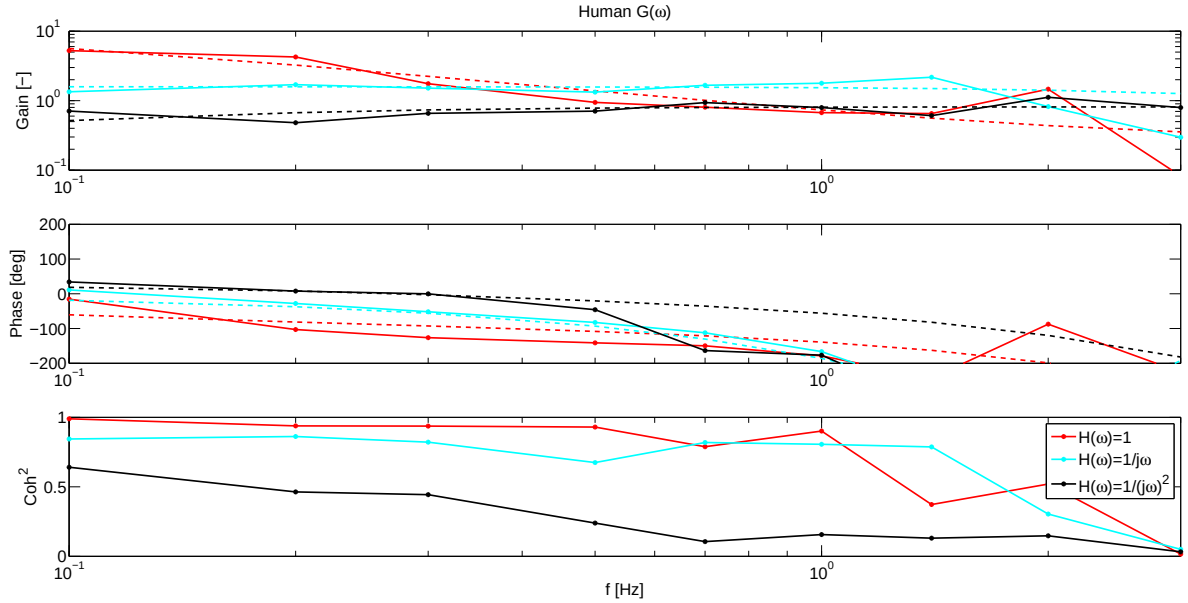


Figure B.19: Magnitude, phase and coherence estimated from spectral densities (—) and crossover model(- -)

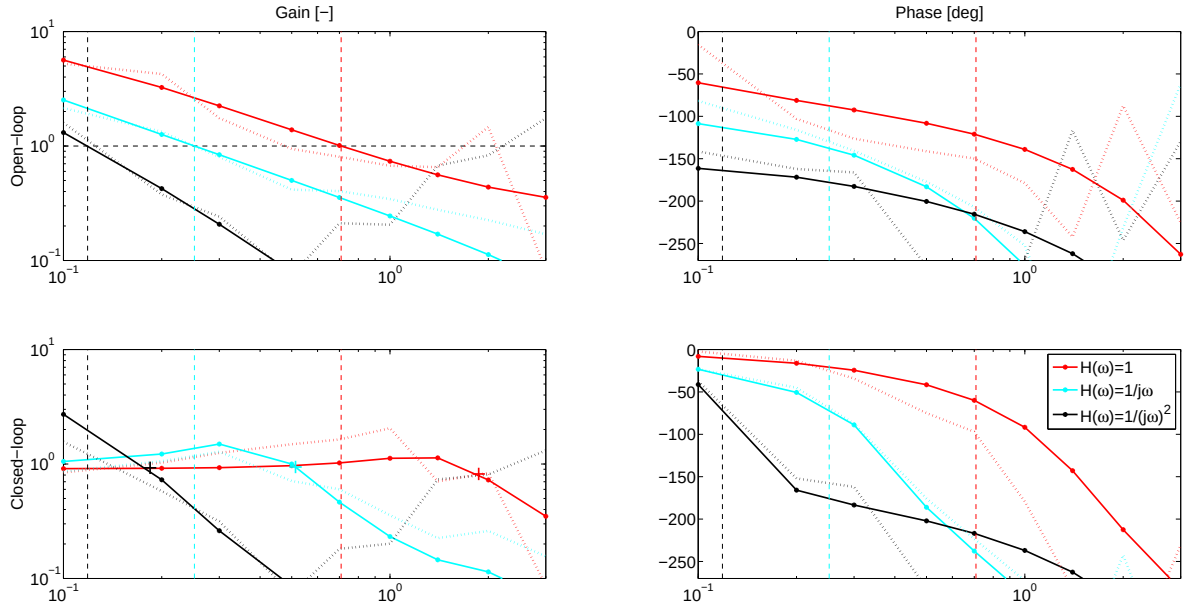


Figure B.20: Crossover frequency (- -) and cutoff frequency (+)

Subject 11

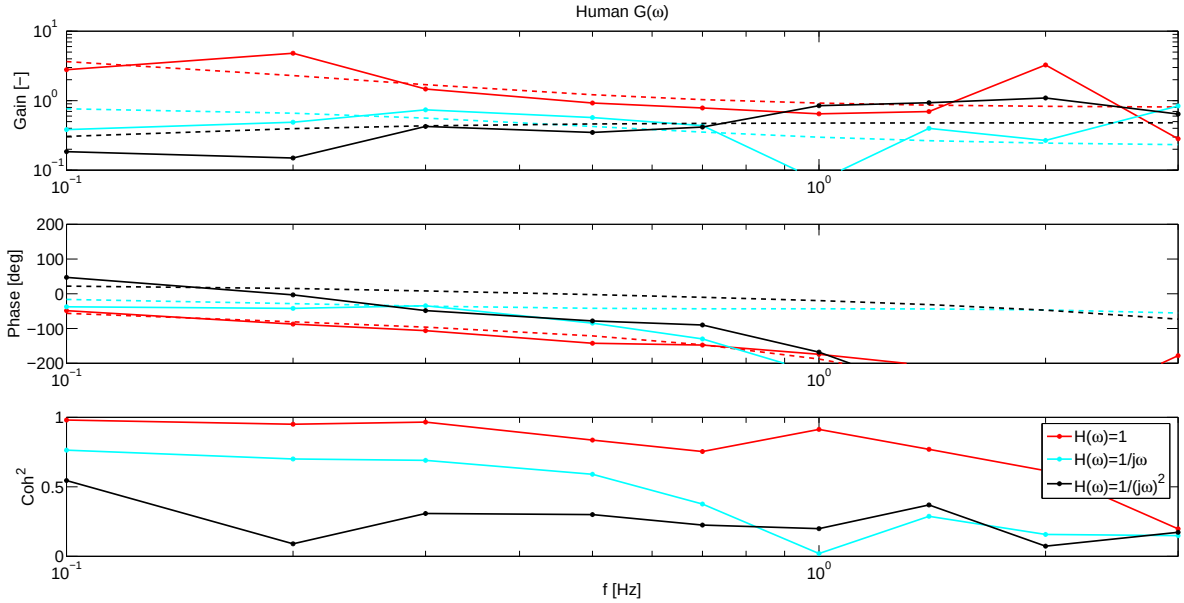


Figure B.21: Magnitude, phase and coherence estimated from spectral densities (—) and crossover model(- -)

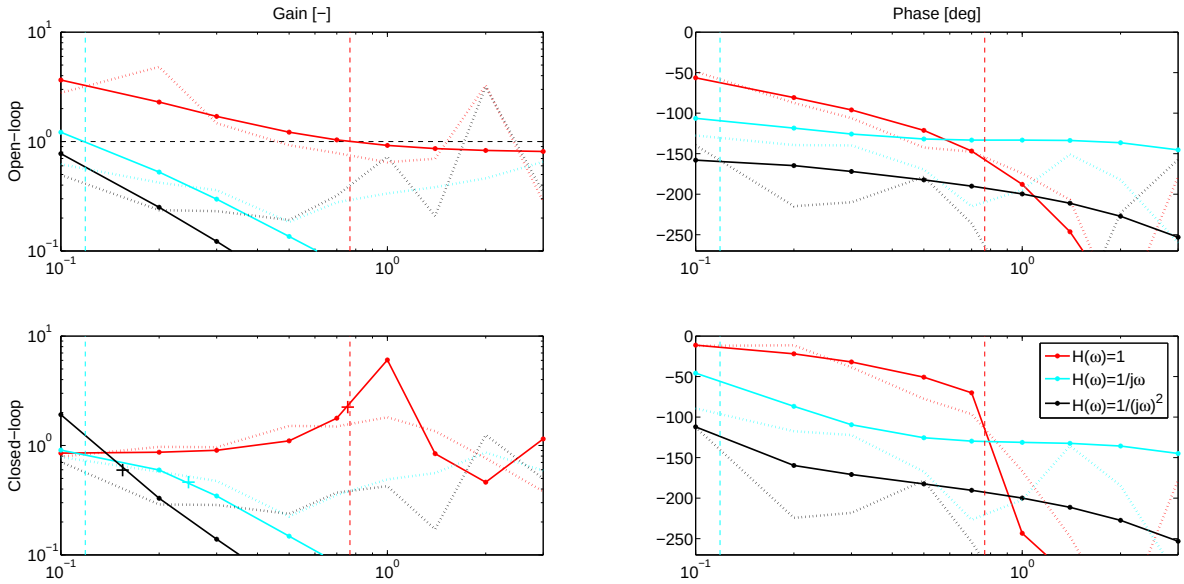


Figure B.22: Crossover frequency (- -) and cutoff frequency (+)

Subject 12

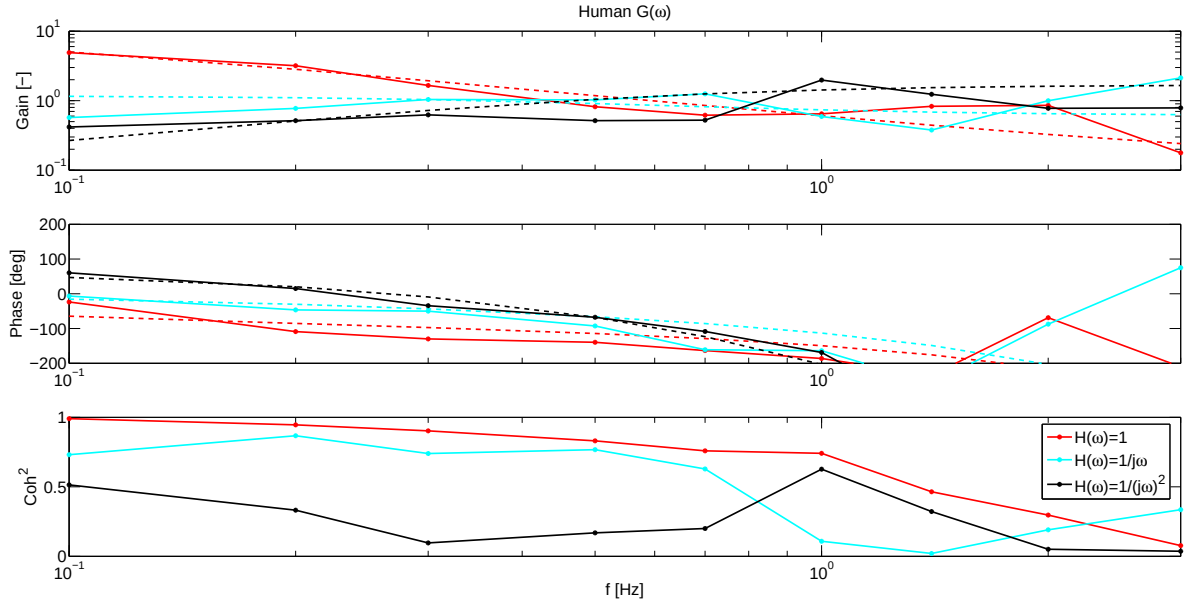


Figure B.23: Magnitude, phase and coherence estimated from spectral densities (—) and crossover model(- -)

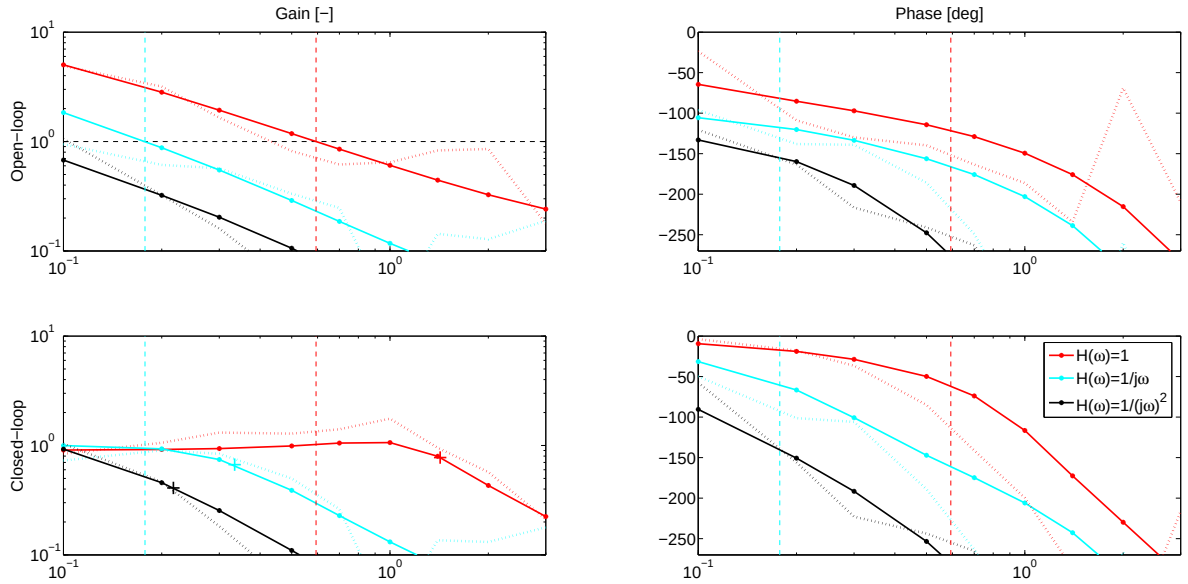


Figure B.24: Crossover frequency (- -) and cutoff frequency (+)

Subject 13

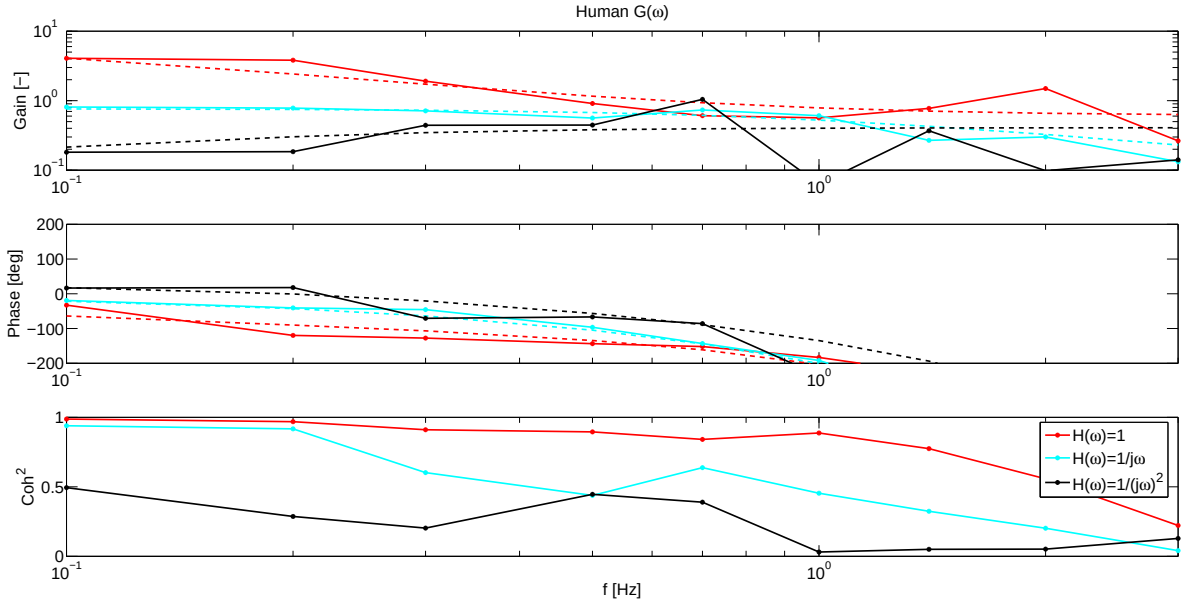


Figure B.25: Magnitude, phase and coherence estimated from spectral densities (—) and crossover model(- -)

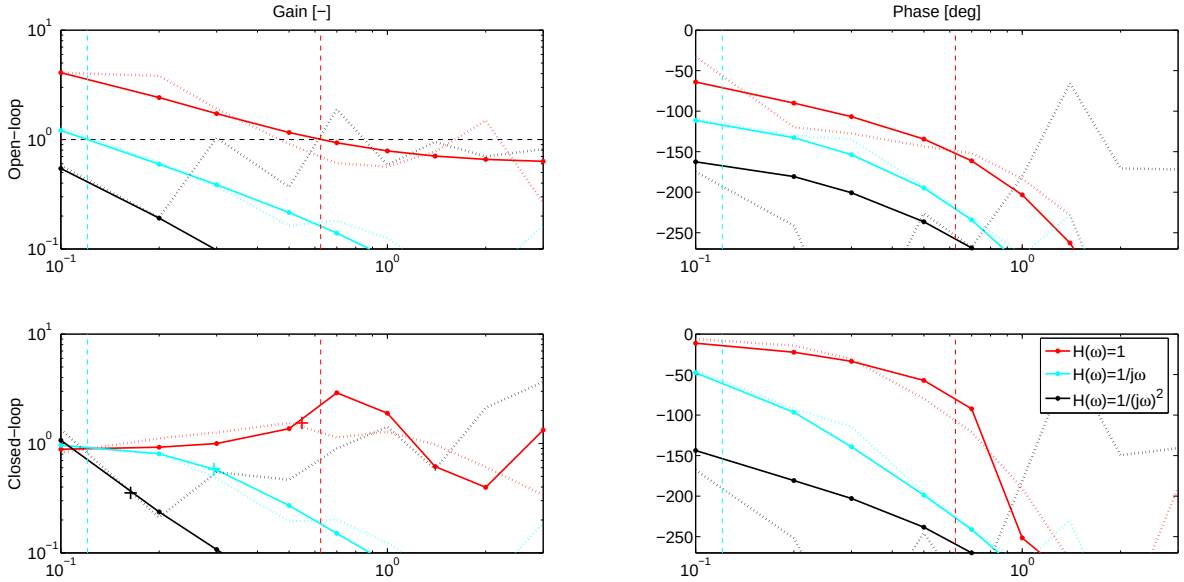


Figure B.26: Crossover frequency (- -) and cutoff frequency (+)

Subject 14

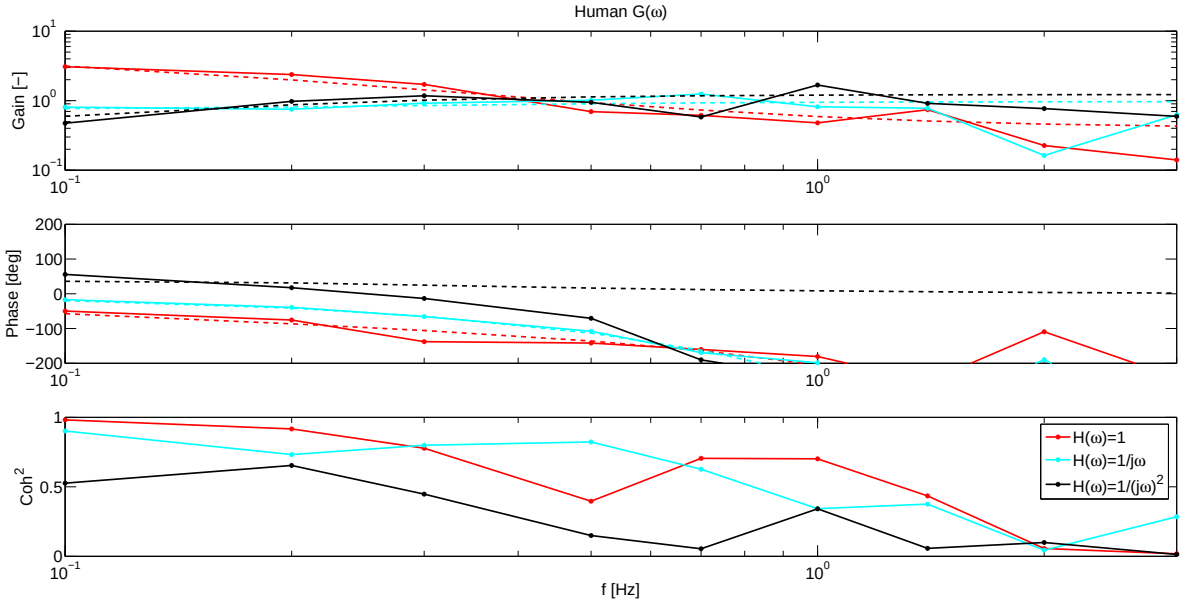


Figure B.27: Magnitude, phase and coherence estimated from spectral densities (—) and crossover model(- -)

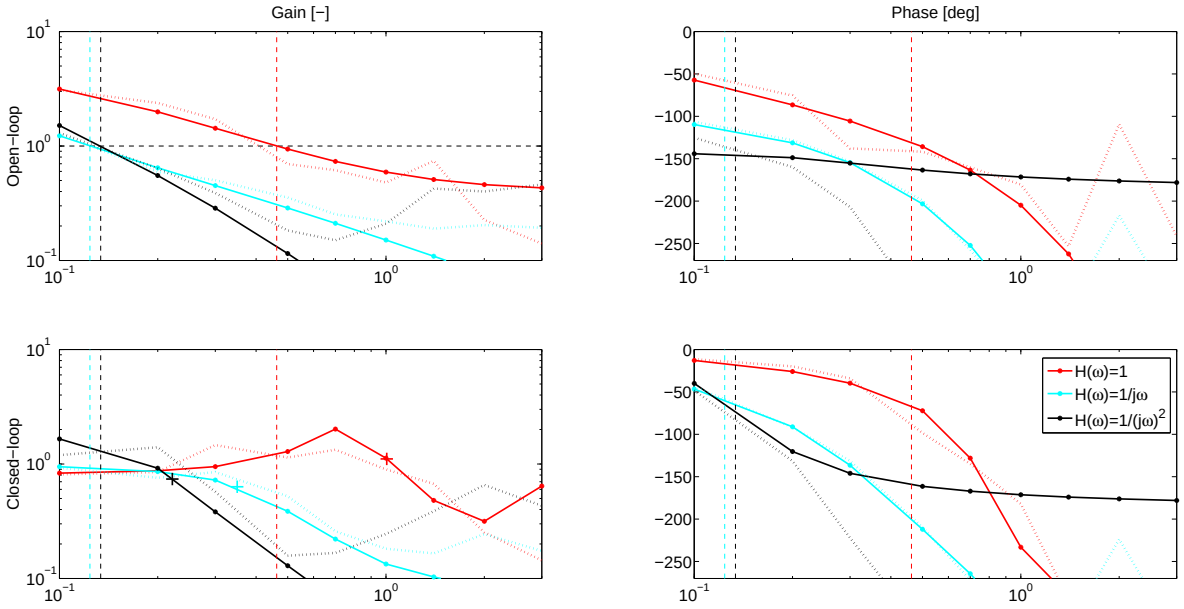


Figure B.28: Crossover frequency (- -) and cutoff frequency (+)

Subject 15

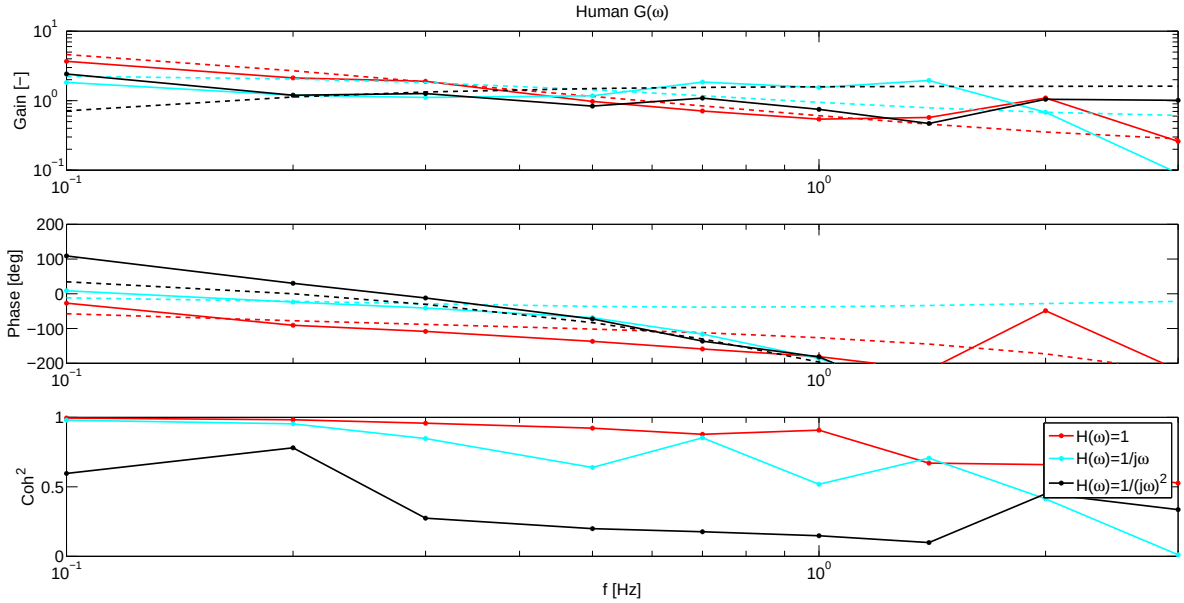


Figure B.29: Magnitude, phase and coherence estimated from spectral densities (—) and crossover model(- -)

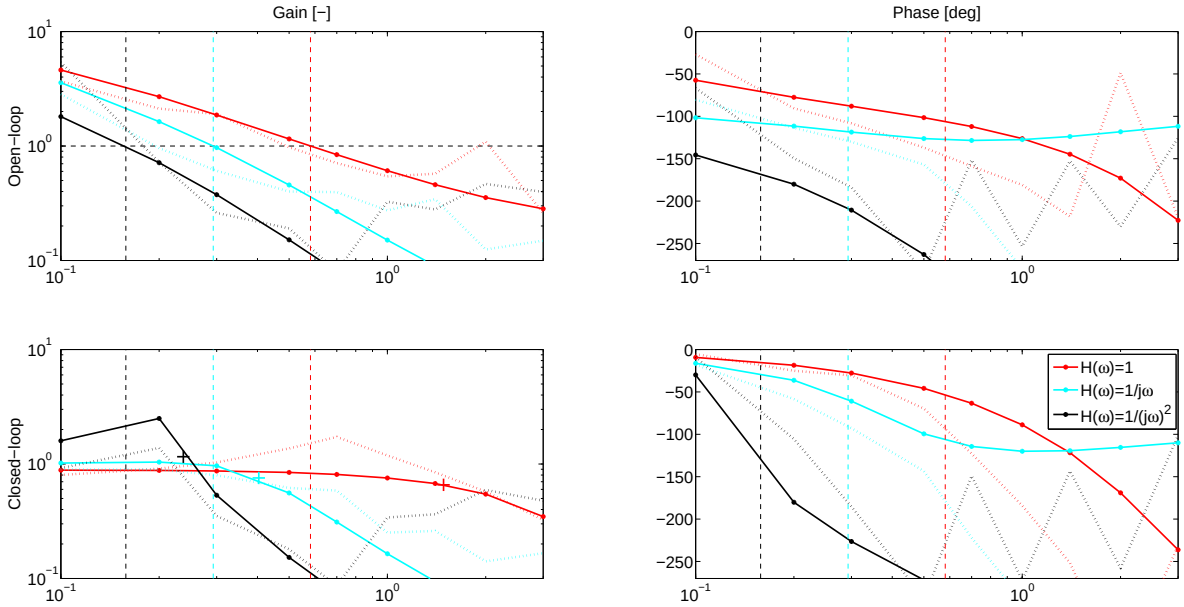


Figure B.30: Crossover frequency (- -) and cutoff frequency (+)

Subject 16

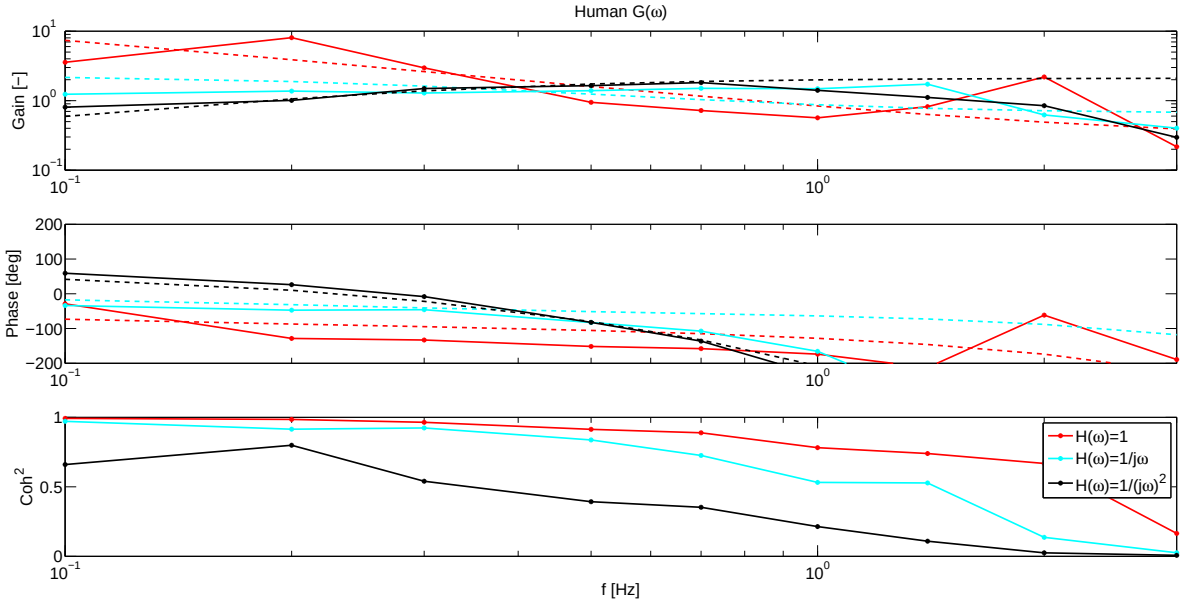


Figure B.31: Magnitude, phase and coherence estimated from spectral densities (—) and crossover model(- -)

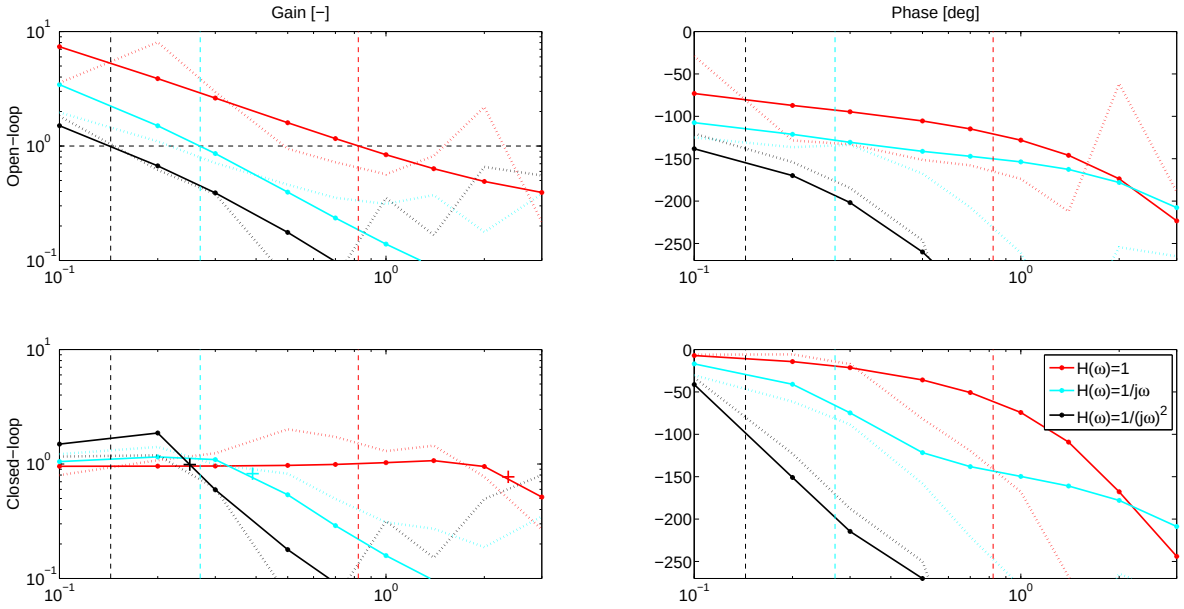


Figure B.32: Crossover frequency (- -) and cutoff frequency (+)

Subject 17

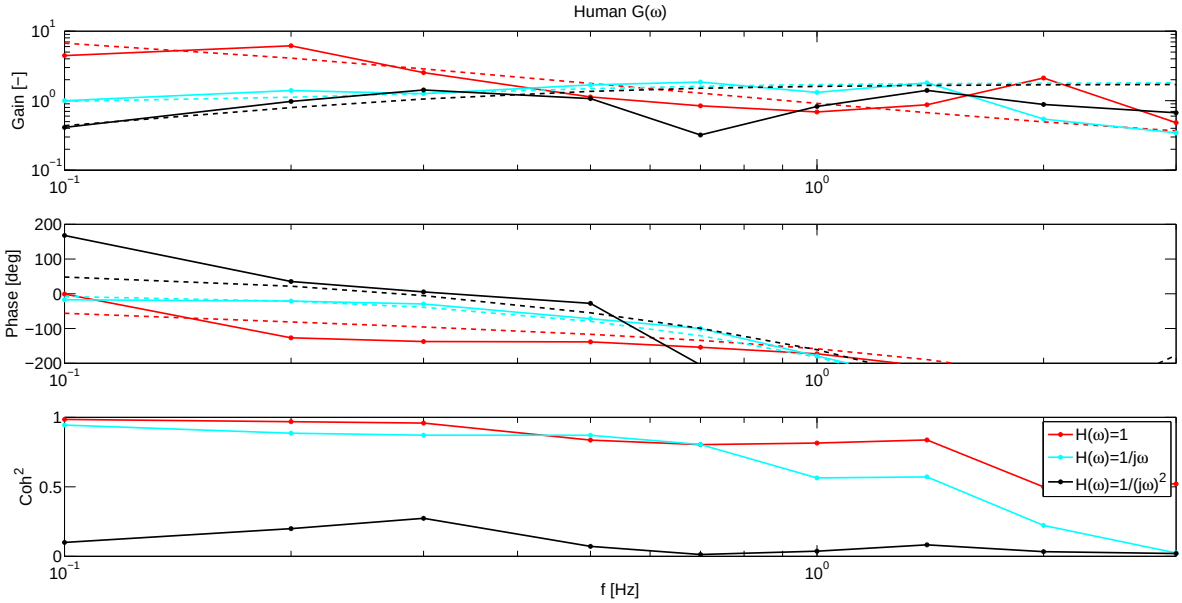


Figure B.33: Magnitude, phase and coherence estimated from spectral densities (—) and crossover model(- -)

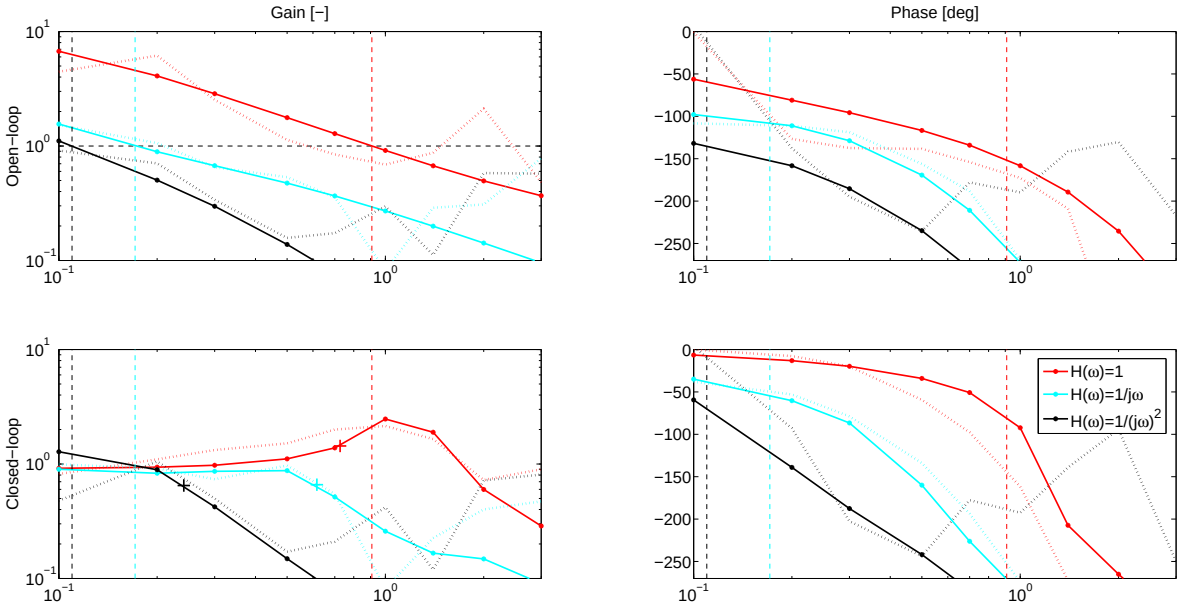


Figure B.34: Crossover frequency (- -) and cutoff frequency (+)

Subject 18

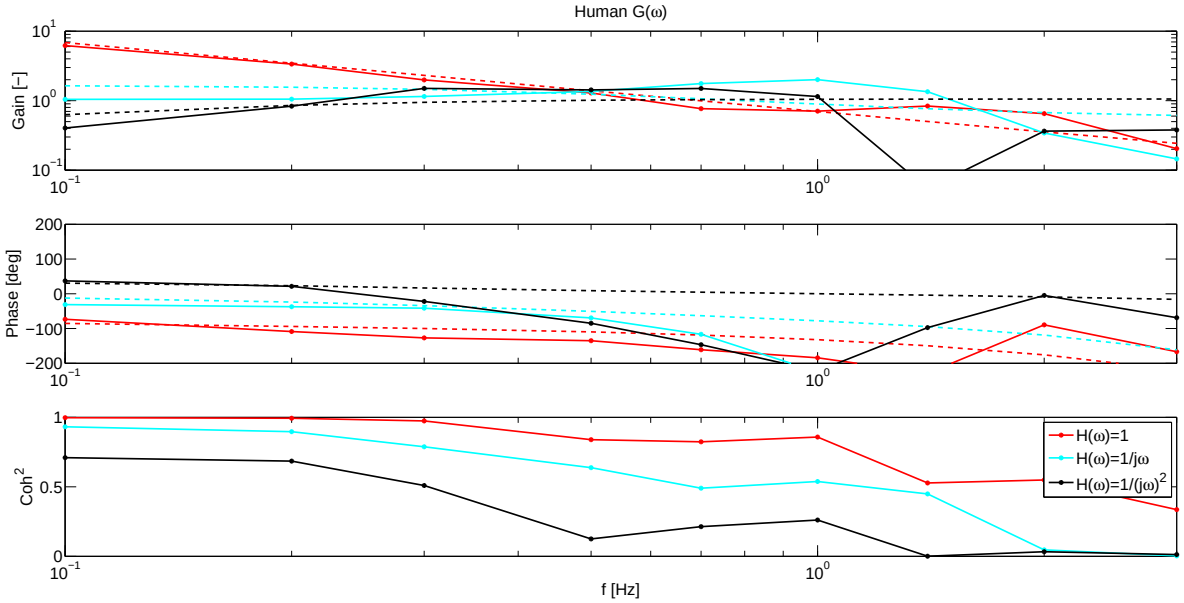


Figure B.35: Magnitude, phase and coherence estimated from spectral densities (—) and crossover model(- -)

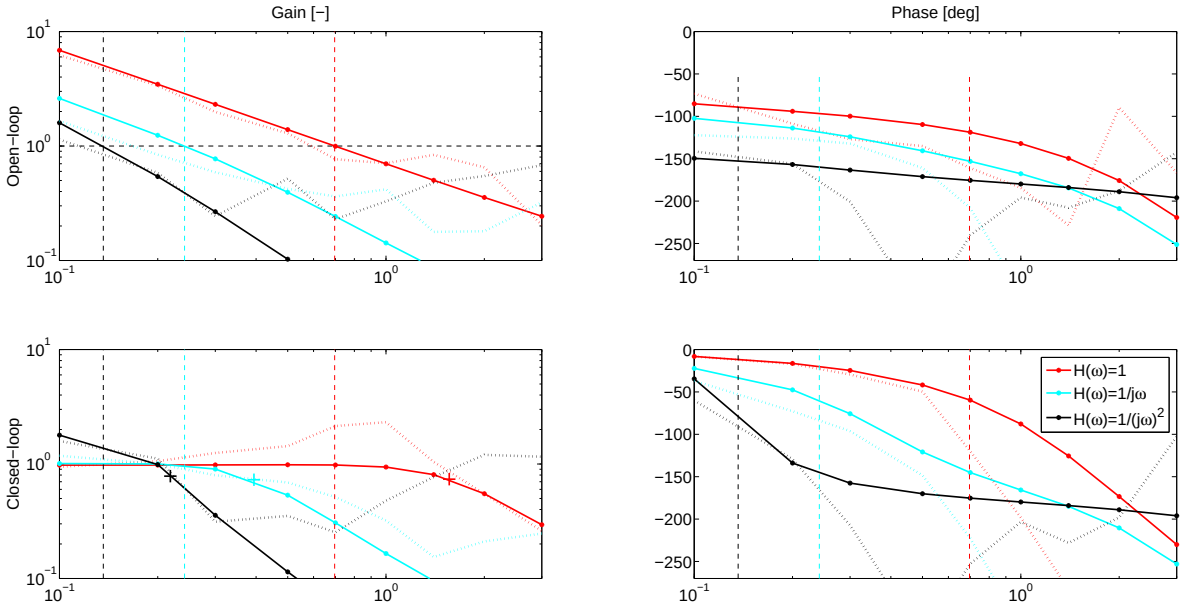


Figure B.36: Crossover frequency (- -) and cutoff frequency (+)

Subject 19

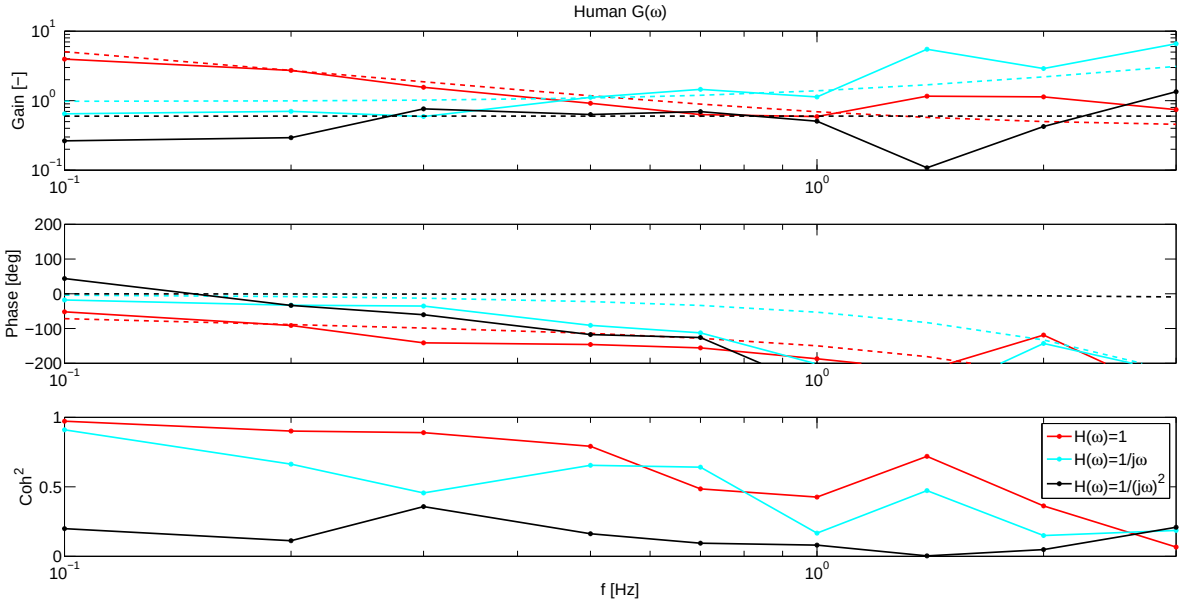


Figure B.37: Magnitude, phase and coherence estimated from spectral densities (—) and crossover model(- -)

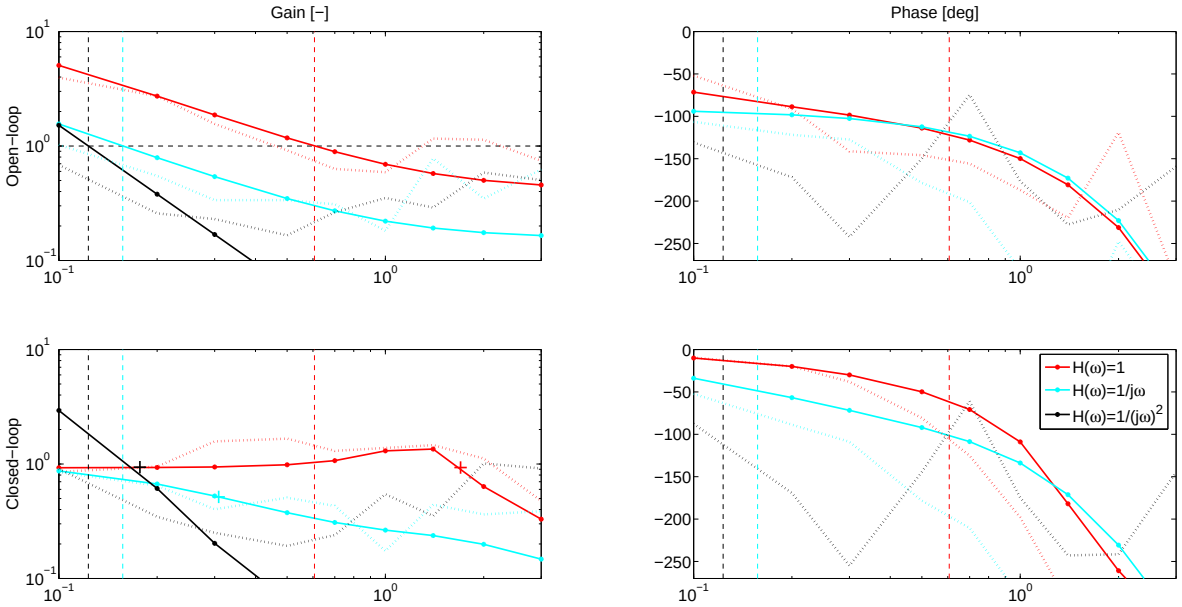


Figure B.38: Crossover frequency (- -) and cutoff frequency (+)

Subject 20

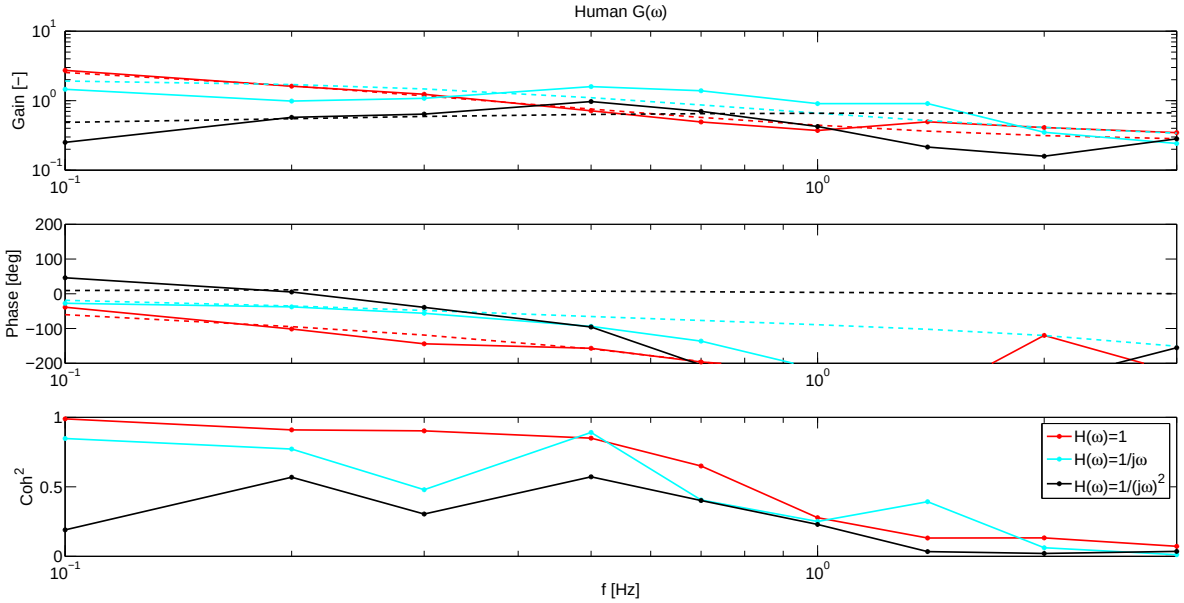


Figure B.39: Magnitude, phase and coherence estimated from spectral densities (—) and crossover model(- -)

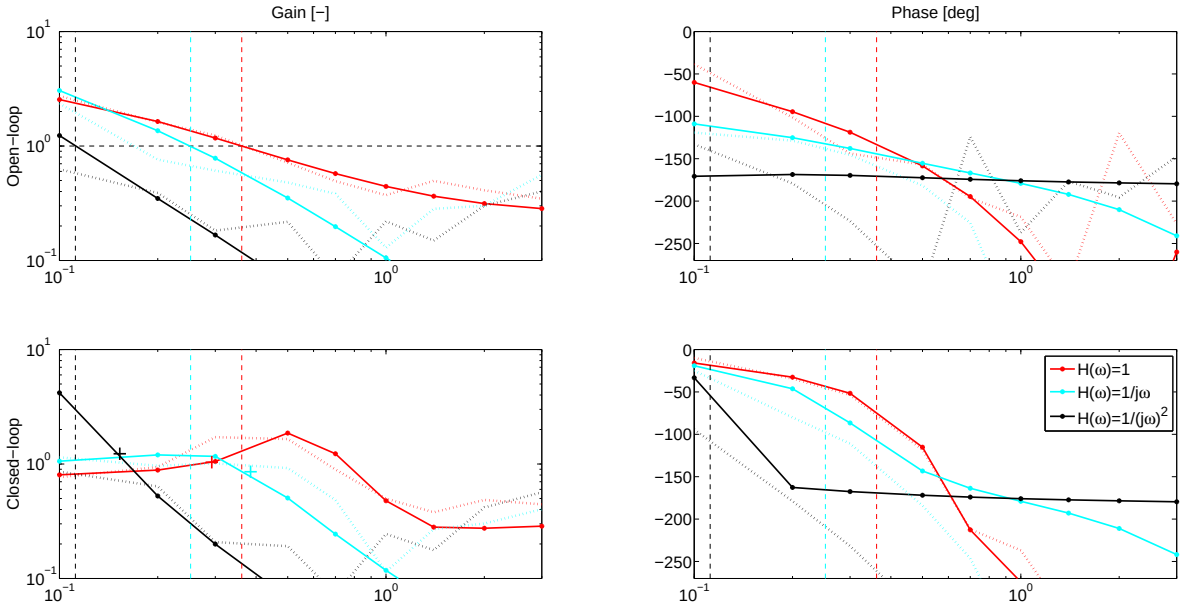


Figure B.40: Crossover frequency (- -) and cutoff frequency (+)

Subject 21

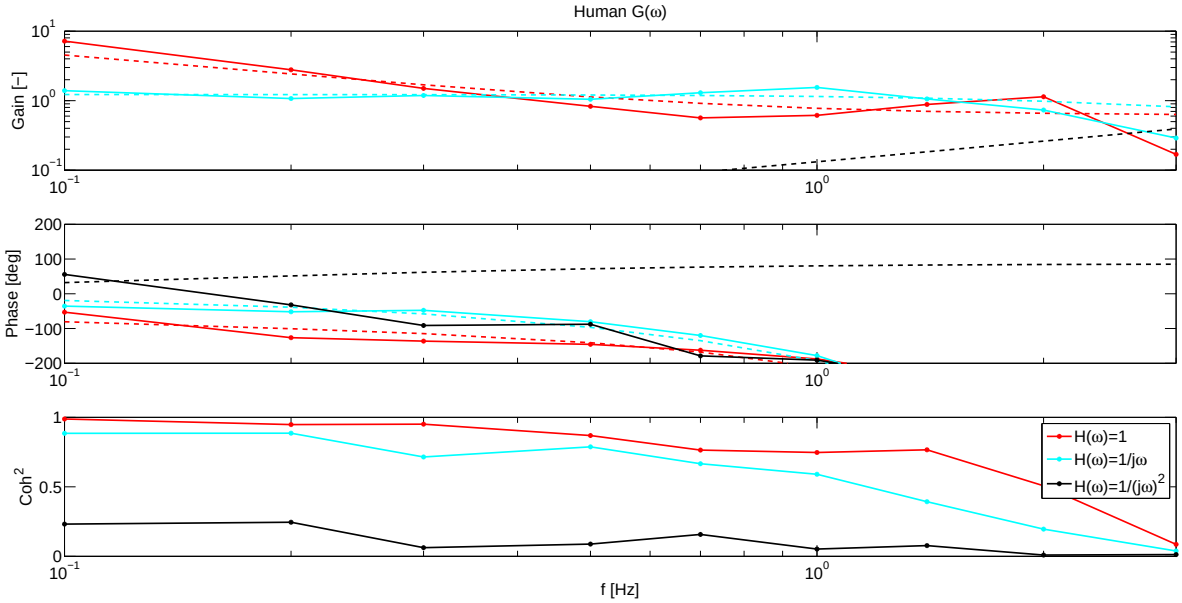


Figure B.41: Magnitude, phase and coherence estimated from spectral densities (—) and crossover model(- -)

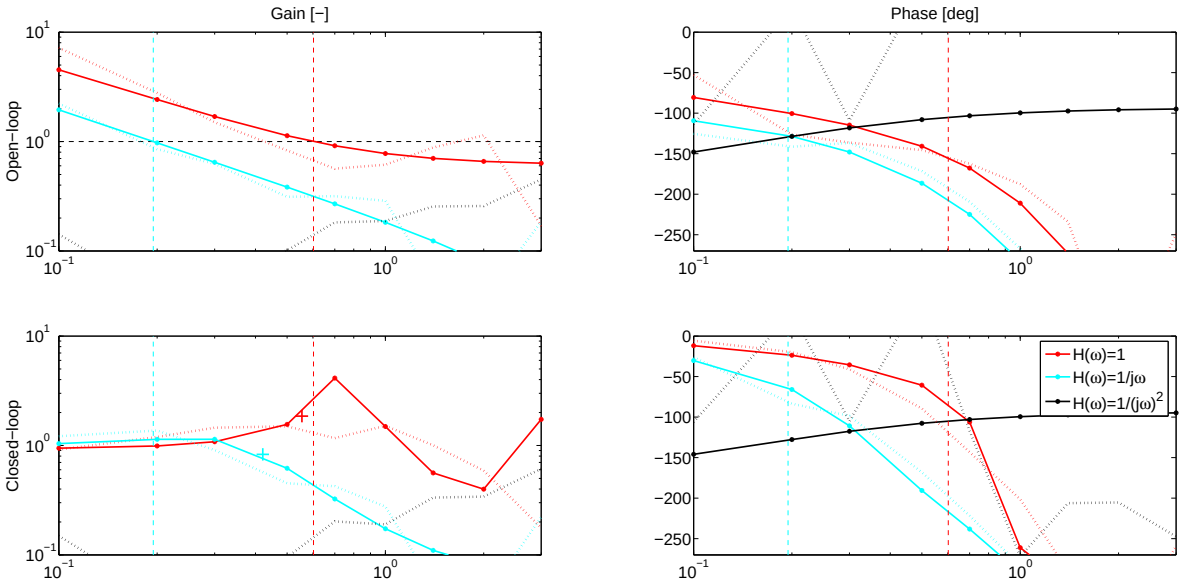


Figure B.42: Crossover frequency (- -) and cutoff frequency (+)

C

Test-retest parameter values

Table C.1: This table shows the means and the standard deviation of the estimated parameters, the crossover and cuttoff frequencies (n=9).

$H(\omega)$	Test #	$K[-]$	(SD)	$\tau_{lead}[s]$	(SD)	$\tau_{lag}[s]$	(SD)	$\tau_e[s]$	(SD)
1	1	13.83	(10.53)	0.11	(0.06)	3.60	(2.38)	0.30	(0.13)
	2	8.83	(5.09)	0.10	(0.06)	2.27	(0.80)	0.31	(0.13)
	3	15.97	(15.08)	0.06	(0.05)	4.08	(3.43)	0.25	(0.13)
$\frac{1}{j\omega}$	1	1.52	(0.57)	0.20	(0.31)	0.36	(0.24)	0.28	(0.21)
	2	1.41	(0.47)	0.17	(0.32)	0.24	(0.15)	0.29	(0.19)
	3	1.54	(0.57)	0.16	(0.32)	0.31	(0.22)	0.29	(0.22)
$\frac{1}{(j\omega)^2}$	1	0.15	(0.11)	5.59	(3.43)	0.47	(0.32)	0.41	(0.28)
	2	0.20	(0.12)	5.32	(2.98)	0.78	(0.32)	0.24	(0.26)
	3	0.29	(0.23)	4.24	(3.35)	0.69	(0.37)	0.41	(0.50)

$H(\omega)$	Test #	$\omega_c[Hz]$	(SD)	$GX[Hz]$	(SD)
1	1	0.62	(0.13)	1.52	(0.52)
	2	0.64	(0.17)	1.37	(0.54)
	3	0.58	(0.10)	1.37	(0.46)
$\frac{1}{j\omega}$	1	0.22	(0.05)	0.40	(0.08)
	2	0.21	(0.06)	0.42	(0.08)
	3	0.22	(0.05)	0.42	(0.08)
$\frac{1}{(j\omega)^2}$	1	0.09	(0.03)	0.20	(0.03)
	2	0.11	(0.02)	0.20	(0.03)
	3	0.11	(0.03)	0.20	(0.04)

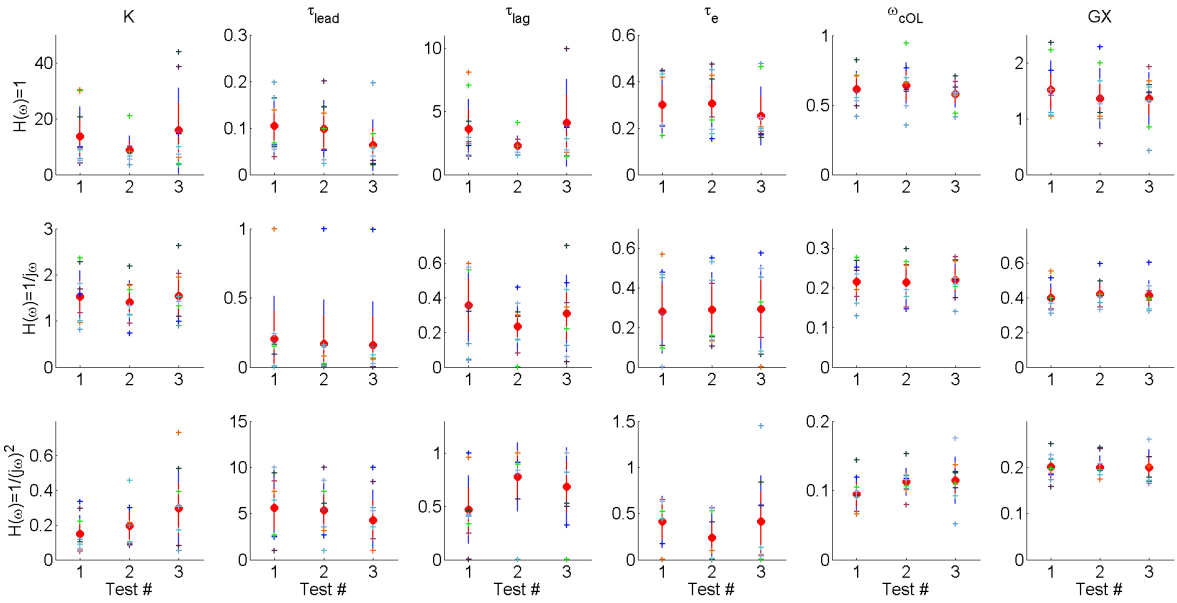


Figure C.1: The values of the estimated parameters the crossover and cuttoff frequencies of test 1, 2 and 3. The box-plot shows the mean and standard deviation per test and the +-signs represent the values of the parameters for each subject. *One should be aware that the y-axes are all different.*